SKB

TECHNICAL REPORT 94-29

Heat conductivity of buffer materials

Lennart Börgesson, Anders Fredrikson,
Lars-Erik Johannesson

Clay Technology AB, Lund, Sweden

November 1994

SVENSK KÄRNBRÄNSLEHANTERING AB
SWEDISH NUCLEAR FUEL AND WASTE MANAGEMENT CO

BOX 5864 S-102 40 STOCKHOLM
TEL. 08-665 28 00 TELEX 13108 SKB
TELEFAX 08-661 57 19

HEAT CONDUCTIVITY OF BUFFER MATERIALS

Lennart Börgesson, Anders Fredrikson,
Lars-Erik Johannesson

Clay Technology AB, Lund, Sweden

November 1994

HEAT CONDUCTIVITY OF BUFFER MATERIALS

Lennart Börgesson
Anders Fredrikson
Lars-Erik Johannesson

Clay Technology AB
Lund
Sweden

November 15, 1994

Keywords: bentonite, buffer material, field tests, heat conductivity, laboratory tests, thermal conductivity,

ABSTRACT (English)

The report deals with the thermal conductivity of bentonite based buffer materials. An improved technique for measuring the thermal conductivity of buffer materials is described. Measurements and FLAC calculations applying this technique have led to a proposal of how standardized tests should be conducted and evaluated. The thermal conductivity of bentonite with different void ratio and degree of water saturation has been determined in the following different ways:

- Theoretically according to three different investigations by other researchers.
- Laboratory measurements with the proposed method.
- Results from back-calculated field tests

Comparison and evaluation showed that these results agreed very well, when the buffer material was almost water saturated. However, the influence of the degree of saturation was not very well predicted with the theoretical methods. Furthermore, the field tests showed that the average thermal conductivity in situ of buffer material (compacted to blocks) with low degree of water saturation was lower than expected from laboratory tests.

ABSTRACT (Swedish)

Rapporten handlar om bestämning av termisk konduktivitet på bentonit-baserade buffertmaterial. En teknik för laboratoriebestämning av termisk konduktivitet på buffertmatarial, som vidareutvecklats i detta projekt, beskrivs i rapporten. Laboratoriemätningar och FLAC-beräkningar av metoden har resulterat i ett förslag till testnings- och utvärderingsmetodik. Den termiska konduktiviteten hos bentonit med olika portal och vattenmättnadsgrad har bestämts på tre olika sätt och resultaten jämförs och diskuteras. Följande metoder har använts för dessa bestämningar:

- Teoretiskt enligt förslag från tre olika forskare.
- Laboratoriebestämningar med den föreslagna metodiken.
- Fältförsök där de mätta temperaturerna har omräknats till värmeledningstal.

Utvärdering och jämförelse mellan metoderna visade på god överensstämmelse när buffermaterialet var vattenmättat eller nästan vattenmättat. Emellertid stämde den teoretiska beräkningen av vattenmättnadsgradens inflytande ganska dåligt överens med den uppmätta. Dessutom visade resultaten från fälttesterna att medelvärmeledningstalet hos buffertmaterial i fält med låg vattenmättnadsgrad (kompakterad till block) blev lägre än förväntat från laboratorieförsöken p.g.a. spalterna mellan blocken och sprickbildningar i blocken.

TABLE OF CONTENTS

SUMMARY

The thermal conductivity of the buffer material is an important parameter for the design of a repository. This report deals with the methodology for determining the thermal conductivity of buffer materials and the influence of void ratio, degree of saturation and field conditions.

A litterature survey has yielded three proposed methods for theoretical determination of the thermal conductivity. A technique for laboratory determination of the thermal conductivity with a thermal probe has been further developed and investigated by making FLAC-calculations. A test and evaluation methodolgy based on these calculations is proposed in the report. Several series of laboratory tests on bentonite with different void ratio and degree of water saturation have been performed and the results have been compared with the theoretical values. Three field tests in the Stripa mine have been used for checking the influence of field conditions on the heat conductivity. These tests have been calculated by use of the finite element method and the resulting thermal conductivity of the buffer material in the field has been evaluated from back-calculations of these results and compared to the theoretical values.

The measured thermal conductivity falls within the scatter of data obtained by using the theoretical relations and the influence of a change in void ratio, which is quite small, can be estimated according to an average of the theoretically deduced expressions. However, the influence of a change in degree of water saturation, which is rather large, is not very well described by the theoretical methods and it is proposed that the measured relation at the void ratio 0.8 should be used. The result from the field tests show that the laboratory derived and theoretically determined values are applicable under field conditions if the degree of water saturation is very high. However, they also show that the back-calculated values at a low degree of water saturation are lower than expected, probably due to the slots between the blocks and cracks and inhomogeneous conditions resulting from moisture redistribution.

All tests and back-calculations of Mx-80 buffer material with a degree of saturation higher than 90% and a density between 1.9 t/m^3 and 2.1 t/m^3 resulted in values of the thermal conductivity between 1.25 W/m,K and 1.35 W/m,K.

1 INTRODUCTION

The thermal conductivity of the buffer material embedding the waste canisters in HLW repositories has an impact on the maximum thermal load that can be applied in the canisters in order to keep the maximum temperature in the buffer material below a certain value. Optimum design of the repository requires a well known value of the thermal conductivity while the heat capacity is less important and can be neglected. (Svemar & Börgesson, 1993).

Several investigations of the thermal properties of bentonite-based materials have been reported and several methods, theoretical as well as laboratory-based, for determining the thermal conductivity have been proposed. However, the results from these investigations vary a lot and there is an urgent need for more accurate determinations. The aim of the present project has been the following:

- to develop a simple and reliable technique for measuring the heat conductivity of buffer and backfill materials
- to determine the heat conductivity of a number of highly compacted blocks of Mx-80 Na-bentonite with different void ratios and degrees of saturation
- to compare the recorded values with measurements reported by others and also with theoretically deduced data
- to evaluate the heat conductivity from back-calculations of field tests and compare these values with the laboratory determined values and the theoretical relations

There are several reasons for comparing laboratory measurements with field measurements since the thermal behaviour in the field and in the laboratory may be quite different. The main differences are:

1. The degree of saturation may be different in different parts of a buffer mass and may change with time in the field.
2. There may be an influence of other mechanisms on the thermal transport like convection, radiation and evaporation-condensation especially before water saturation is reached.
3. Air-filled gaps between individual blocks and between blocks and the canister or the rock will strongly influence the thermal transport.
4. The heat transfer between the canister and the bentonite may affect the thermal transport.

5. The influence of swelling pressure and temperature is not considered in normal laboratory tests.

The purpose of this project has thus been to develop a technique for obtaining relevant values of the heat conductivity of bentonite-based buffer and backfill material and to get typical values for the range of void ratio and degree of water saturation that are typical of the buffer in a repository. The following steps have been taken in this project:

- A suvey of some earlier investigations of the thermal properties of highly compacted clay based buffer materials.
- Development of the probe method with transient heat flow for measuring the heat conductivity.
- Theoretical calculations with FLAC of the heat flow at probe testing in order to develop a proper evaluation technique and find the limitations of the method.
- Some test series for measuring the heat conductivity with the probe method.
- Backcalculation of the actual heat conductivity in situ for some field tests.
- Evaluation of the method and recommendation of how to make relevant measurements.

2 EARLIER INVESTIGATIONS AND SOME THEORETICAL ASPECTS

Numerous investigations of the thermal conductivity λ of different soils have been made (e.g. Farouki 1986). Many of these investigations have resulted in proposed theoretical formulas for calculations of λ based on empirical data and more or less coupled to the real processes. Three of the investigations, which have concerned buffer material, will be briefly presented.

Investigation by Kahr & Müller-von Moos (1982)

In this investigation, laboratory tests were made on compacted Mx-80 Na-bentonite and Montigel Ca-bentonite with water ratios between 0% and 12% and bulk densities between 1.4 t/m^3 and 2.3 t/m^3 corresponding to the void ratio $0.29<e<1.1$ and degree of saturation $0\%<S_r<82\%$ where

e = pore volume divided to the volume of solids
S_r = pore volume filled with water divided to the total pore volume

The thermal conductivity was determined with a technique resembling the one used at Clay Technology AB (CT).

The measured heat conductivity λ varied between 0.4 and 1.3 W/m,K. No significant difference was found between experimentally determined λ-values and values deduced by use of Eqn 2-1, which empirically describes the relation between the heat conductivity, the bulk density ρ and the water ratio w with an accuracy of about +/- 0.1 W/m,K.

$$\lambda = 0.56 + 0.60\rho + 0.4\rho^3 w/(w+1) \qquad (2\text{-}1)$$

where ρ = total weight of bentonite and water divided by the volume
w = weight of water divided by the weight of the dry material

The influence of temperature was determined on completely dry samples and was found to increase with temperature T(°C) according to Eqn 2-2.

$$\Delta\lambda = 0.01 \cdot (\Delta T)^{0.5} \qquad (2.2)$$

If this influence is valid also for bentonite close to water saturation, it means that λ will be 0.08 W/m,K higher at the maximum temperature in a repository than at room temperature in the laboratory.

Investigation by Beziat et al. (1988)

This investigation was made in order to study the heat conductivity of the French natural clay Fo-Ca which is also the French reference clay for buffer material. It was found that the geometric mean model for porous media (Woodside and Messmer, 1961) according to Eqn 2-3 gave values that agreed fairly well with the measured ones.

$$\lambda = \lambda_s^{1-n} \cdot \lambda_w^{n \cdot S_r} \cdot \lambda_a^{n \cdot (1-S_r)} \qquad (2\text{-}3)$$

where λ_s = heat conductivity of solids = 2.6 W/m,K
λ_w = heat conductivity of water = 0.6 W/m,K
λ_a = heat conductivity of air = 0.024 W/m,K
n = porosity (pore volume divided to total volume)
n = $e/(1+e)$
S_r = degree of saturation %

The value of λ_s = 2.6 W/m,K was found to give the best agreement with the measured values and it coincides well with what is considered to be an average of soil minerals containing an insignificant amount of quartz. Good agreement between the calculated and measured values were obtained for clay with a void ratio e varying between 0.45 and 1.5 at the water ratios 5% and 11%, corresponding to $10\% < S_r < 65\%$, and the measured heat conductivities varied from 0.2 W/m,K to 1.1 W/m,K. The accuracy in this investigations was about +/- 0.2 W/m,K.

Investigation by Knutsson (1983)

Knutsson investigated the thermal properties of highly compacted pure Mx-80 bentonite. The tests were made by using a very thin metal film confined between two samples of bentonite. This technique has the advantage that the test can be performed under different external pressures and in the course of the water uptake process, i.e. with different swelling pressures, as well as at different temperatures. However, the disadvantages were found to be that the technique was very complicated and that the film easily broke during the tests, which resulted in very few successful recordings. The technique is not recommended for practical use.

Knutsson found that Johansen's method (Johansen & Frivik, 1980) for calculating the thermal conductivity were applicable to highly compacted bentonite. According to this method the thermal conductivity λ can be calculated by Eqns 2-4 to 2-7.

$$\lambda = \lambda_0 + K_e(\lambda_1 - \lambda_0) \qquad (2\text{-}4)$$

where

$$\lambda_0 = 0.034 \cdot n^{-2.1} \qquad (2\text{-}5)$$

$$\lambda_1 = 0.56^n \cdot 2^{(1-n)} \qquad (2\text{-}6)$$

$$K_e = 1 + \log S_r \qquad (2\text{-}7)$$

where λ_0 = thermal conductivity at $S_r = 0$
λ_1 = thermal conductivity at $S_r = 100\%$
K_e = influence of the degree of saturation S_r
n = porosity

Eqn 2-5 was found to be valid with the accuracy +/- 20%.

The influence of temperature and pressure were also investigated. Eqn 2-8 was found to be valid.

$$\lambda_2/\lambda_1 = 1 + \beta \cdot \Delta T/100 \qquad (2\text{-}8)$$

where λ_2 = thermal conductivity at the higher temperature
λ_1 = thermal conductivity at the lower temperature
ΔT = temperature difference
β = parameter with the value 0.09-0.17

Eqn 2-8 yields the same increase in the thermal conductivity (0.08 W/m,K) at the maximum temperature in a repository as Eqn 2-2.

The heat conductivity was found to increase with increasing pressure with about 0.006 W/m,K per MPa pressure. If this is not an effect of improved contact between the bentonite and the metal film, it means that the thermal conductivity of a water saturated bentonite with the swelling pressure 10 MPa is 0.06 W/m,K higher than measured. The combined effect of temperature and pressure will thus according to this investigation increase the heat conductivity by 0.1-0.15 W/m,K in situ.

Comparison between the three proposals

The three different proposed relations for theoretically calculating the thermal conductivity of bentonite-based buffer materials have yielded good agreement with the laboratory determined values. However, two of them are partly empirical. Only the proposed method by Knutsson is completely neutral in the sense that it is originally derived for other materials. A comparison of the different methods is made in Fig. 2-1 which shows the thermal conductivity λ as a function of the void ratio e at three different degrees of saturation S_r. The figure shows that the scatter between the methods is 0.1-0.3 W/m,K except for S_r=1.0 at low void ratios, where it is 0.5 W/m,K, reflecting the fact that only a few tests were made by Knutsson on completely saturated materials. The figure also shows that λ logically increases with increasing S_r and decreasing e for all methods except for λ_2 (Kahr et al.) between e=0.5 and e=0.3. For this reason the value λ_2=1.39 W/m,K at e=0.3 has been put in brackets.

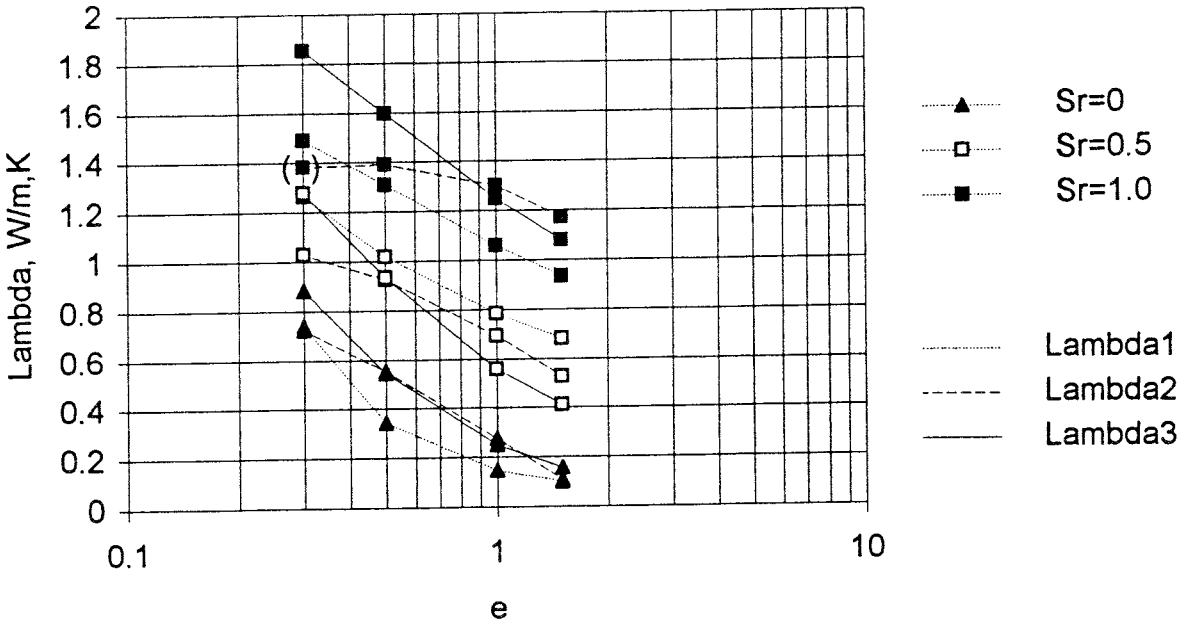

Figure 2-1 Influence of the degree of saturation and the void ratio on the heat conductivity calculated by three different methods.
λ_1 - Knutsson
λ_2 - Kahr et al.
λ_3 - Beziat et al.

Figure 2-2 shows the average values and the scatter of these methods which yield three bands within which the laboratory-determined heat conductivity of pure bentonite blocks should be located. λ_2 at e=0.3 is excluded.

The influence of the degree of saturation on the thermal conductivity calculated according to these three methods is illustrated in Fig 2-3. The calculations have been made for the void ratio e=0.8. The figure clearly shows the inconsistency between the three methods. Although the values do not differ more than 0.2 W/m,K the curve shape is quite different. The slope (the increase in λ with increasing S_r) increases with increasing S_r for λ_1 (Knutsson) while it is almost constant for λ_2 (Kahr et al) and decreases with increasing S_r for λ_3 (Beziat et al).

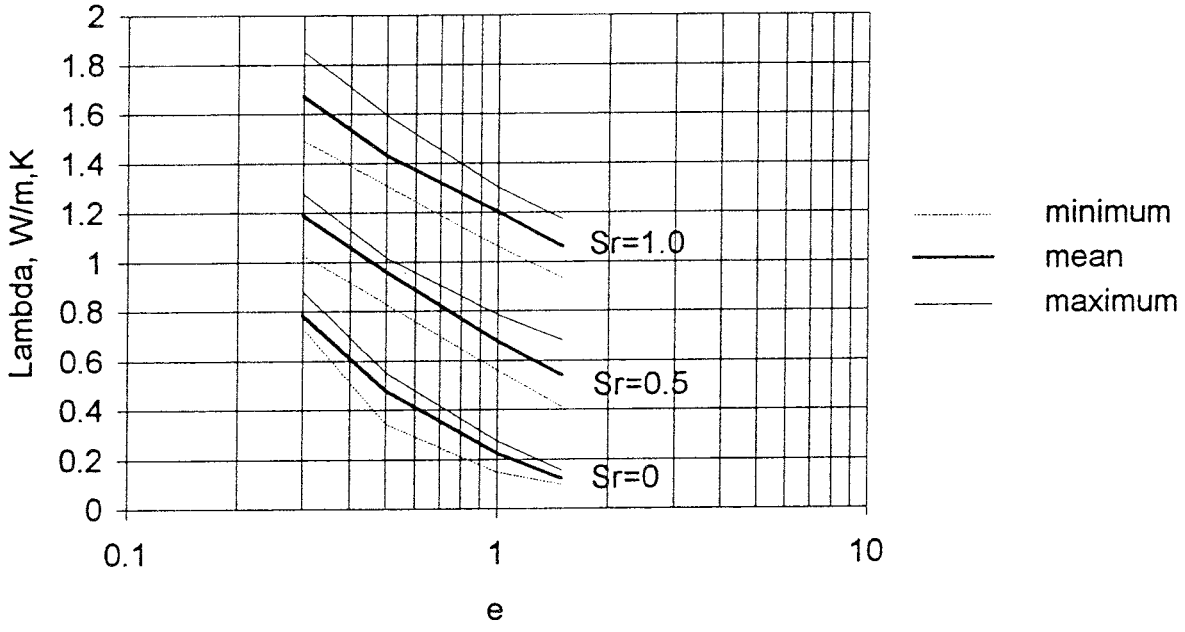

Figure 2-2 The average theoretical heat conductivities calculated from Fig. 2-1 and the span within which all the different methods occur

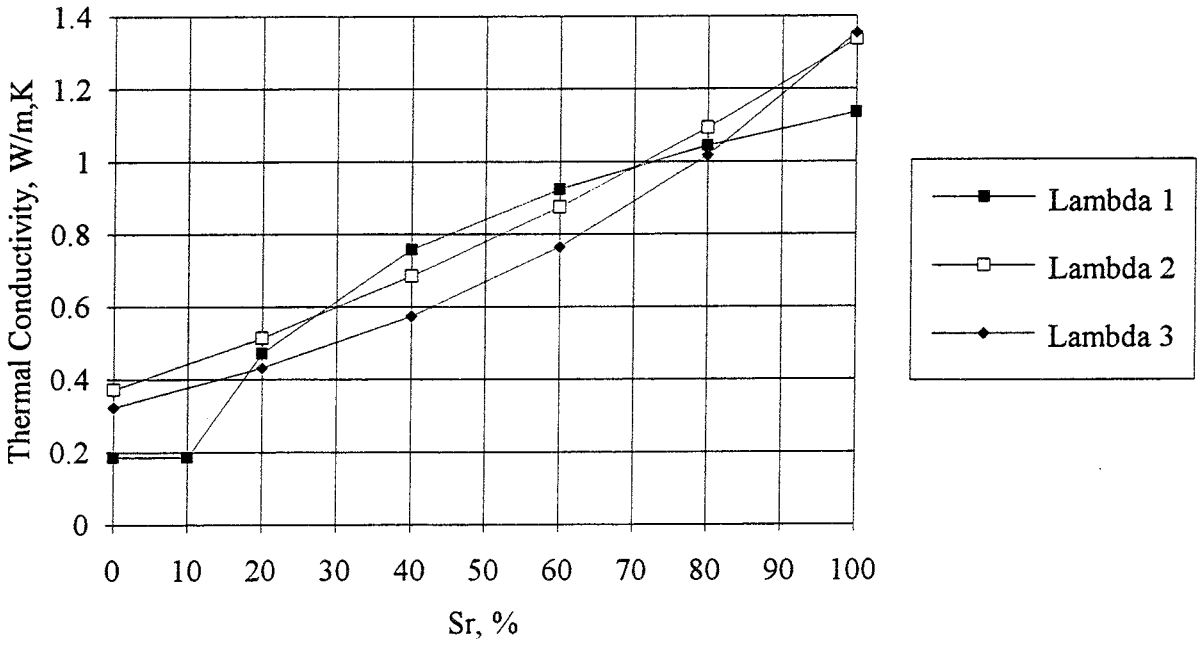

Figure 2-3 Influence of the degree of saturation on the heat conductivity at the constant void ratio $e = 0.8$ according to the three different methods

λ_1 - Knutsson
λ_2 - Kahr et al.
λ_3 - Beziat et al.

3 LABORATORY MEASURING TECHNIQUE

3.1 GENERAL

The most commonly used technique for determining the heat conductivity of materials is to apply a stationary heat flow through the sample. This technique is very accurate but difficult in the sense that it requires a constant thermal gradient in the sample. This is a problem in partially water saturated materials since the heat gradient will cause moisture redistribution in the sample. For this reason, a transient method that requires very short measuring time should be used although it is less accurate.

We have chosen the so called probe method, a "transient" technique that is fairly common in soil testing. The needle-shaped probe with a length that is much larger than the diameter is inserted in the centre of the sample and heated at a constant power. The temperature is measured in the centre of the probe and recorded as a function of time as shown in Fig 3-1. If the length/diameter ratio is large enough, the axial heat conduction can be neglected and the central section modelled as a one-dimensional axial symmetric system. The temperature increase in the probe can be calculated according to Eqn 3-1 if the probe is considered to be a line source (see e.g. Farouki, 1986).

$$T = \frac{-q}{4\pi\lambda} \cdot E_i\left(-\frac{r^2}{4\kappa t}\right) \qquad (3\text{-}1)$$

where

$$E_i(-x) = \int_x^\infty \frac{1}{z} e^{-z} dz \qquad (3\text{-}2)$$

and

T = temperature increase
q = heat flow per meter length
λ = thermal conductivity
r = radius
κ = thermal diffusivity
t = time from start heating

The thermal diffusivity κ is defined according to Eqn 3-3.

$$\kappa = \frac{\lambda}{\rho C_p} \qquad (3\text{-}3)$$

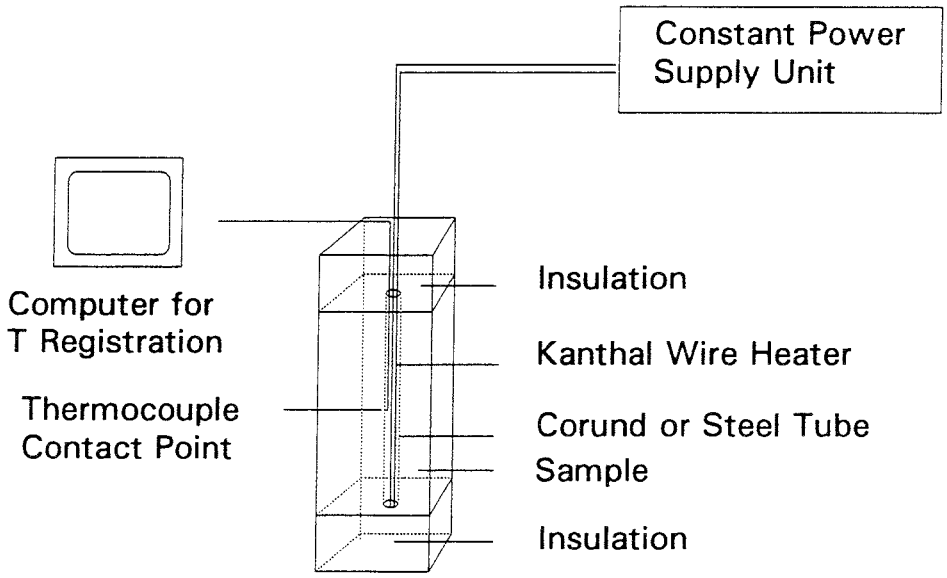

Figure 3-1 Measurement system for determination of thermal conductivity

where

ρ = bulk density
C_p = heat capacity

Eqn 3-1 can be approximated to Eqn 3-4 for high time values and a small radius.

$$T_{t2} - T_{t1} = \frac{q}{4\pi\lambda} \ln \frac{t_2}{t_1} \qquad (3\text{-}4)$$

where

T_{t1} and T_{t2} are the temperature values at the times t1 and t2 respectively.

A real probe differs from the idealized line source by being a cylindrical heat source of finite length, radius, and heat capacity. There is also a contact resistance between the probe and the sample. In spite of this, Eqn 3-4 has been shown to apply within certain limits. Thus, the length/diameter ratio should exceed 25 and the time values must be chosen in a way that neither the contact resistance nor the outer boundaries affect the results.

In the technique developed for testing bentonite samples the probe has penetrated the entire sample and the ends of the sample insulated in order to reduce the axial heat flow.

3.2 EQUIPMENT

The measuring equipment consists of a unit for supply of constant power, the probe, a thermocouple, and a temperature recording unit (a computer data logger) as shown in Fig 3-1. Two different materials have been used for the probe. In the first version of the equipment the probe was made of corundum with "Kanthal" heat wires inserted in axial chanels in the probe. This type of probe was not very good since it broke easily and could not be used more than one time. Also, it was too thick since it had to have a diameter of at least 5 mm. Later, a second version was used with a probe made of stainless steel and the Kanthal wires electically insulated with tephilin tubes. The steel probe was a thin-walled tube with the outer diameter equal to the length 8-10 cm (two versions). The thermocouple was placed in the centre of the steel tube.

3.3 MEASURING TECHNIQUE

The sample dimensions varied in different series. In one series the measurement was made with large blocks with the probe placed at a radial distance of at least 4 cm from the nearest block surface and with an axial distance of several cm between the end of the probe and the bottom surface of the block. In other series the sample was compacted to 10 cm high samples with 5 cm diameter. In a third series the samples were taken from the triaxial apparatus just after a triaxial test and they had a diameter of slightly more than 5 cm and a height of about 8 cm. The influence of the different geometries in these tests have been investigated using FLAC calculations as shown in the next chapter.

The measuring probe is installed in a drilled hole in the sample. The hole should have the same diameter as the probe so that the probe and the sample are in direct contact along the entire surface. In order to improve the contact and minimize the contact resistance the probe was coated with silicon grease before installation. This has turned out be very successful and is much better than the originally tested technique to put water in the hole just before installation.

Most tests have been made using the power 1W applied to the probe. This has turned out to be a good compromise between the desire to have a high power to improve the accuracy of the temperature measurement and the desire to minimize the drying effect of the temperature gradient.

3.4 EVALUATION OF HEAT CONDUCTIVITY

The heat conductivity λ can be calculated using Eqn 3-5, which is a transformation of Eqn 3-4.

$$\lambda = \frac{q}{4\pi\Delta T} \ln \frac{t_2}{t_1} \qquad (3\text{-}5)$$

where

ΔT = temperature increase of the probe in the time interval t_1 to t_2.

The proper time interval for evaluation can be determined if the temperature is plotted as a function of time in a semi-logarithmic diagram. According to Eqn 3-4, this relation should be a straight line and deviation from this shape is caused by boundary effects or changes in properties. They will primarily appear for short testing times, i.e. when the properties of the probe and the contact resistance will dominate the behaviour, and after long time periods when the heating front has reached the outer boundary. Fig 3-2 shows an example of a test plotted in this way. The test was made on a sample of IBECO Na-bentonite with the void ratio e=1.5 and the degree of saturation S_r=98%. The applied power was 1 W and the length of the probe 8 cm. The diagram shows that the temperature curve *T vs. log t* is a straight line between about 50 s and 500 s. If the thermal conductivity is graphically evaluated with the best fitted line for these time values, the result will be:

λ = 1.08 W/m,K

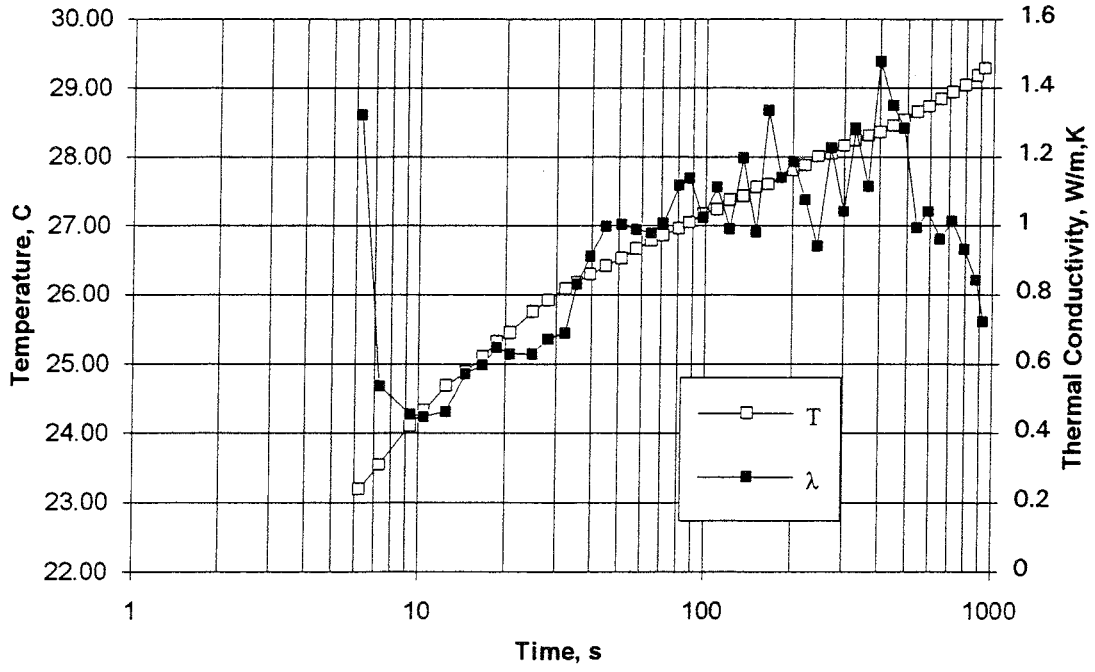

Figure 3-2 Measured temperature T and evaluated thermal conductivity λ from short time intervals

The thermal conductivity can also be calculated by the computer for each pair of recorded data. The results are also plotted in Fig 3-2. The very small time steps make the corresponding change in temperature very small and the influence of the inaccuracy in temperature values very strong. This results in a rather large difference between the evaluated heat conductivity values, which can be seen in the figure by the zigzag pattern of the curve λ *vs.* $\log t$. An attempt to avoid this inconvenience has been made in Fig 3-3, where each temperature value has been calculated as the average of a number of values (requires more frequent logging). The result improves considerably but there is still a considerable scatter. The influence of the accuracy of the temperature measurement is illustrated in the lower diagram in Fig 3-3, in which one temperature value has been deliberately decreased by 0.03°C.

The conclusion is that the thermal conductivity is most accurately evaluated by the graphical technique, which thus yields an average value. However, the technique to calculate the thermal conductivity as a function of time is very helpful for considering the accuracy of the measurement and for estimating the most appropriate time interval.

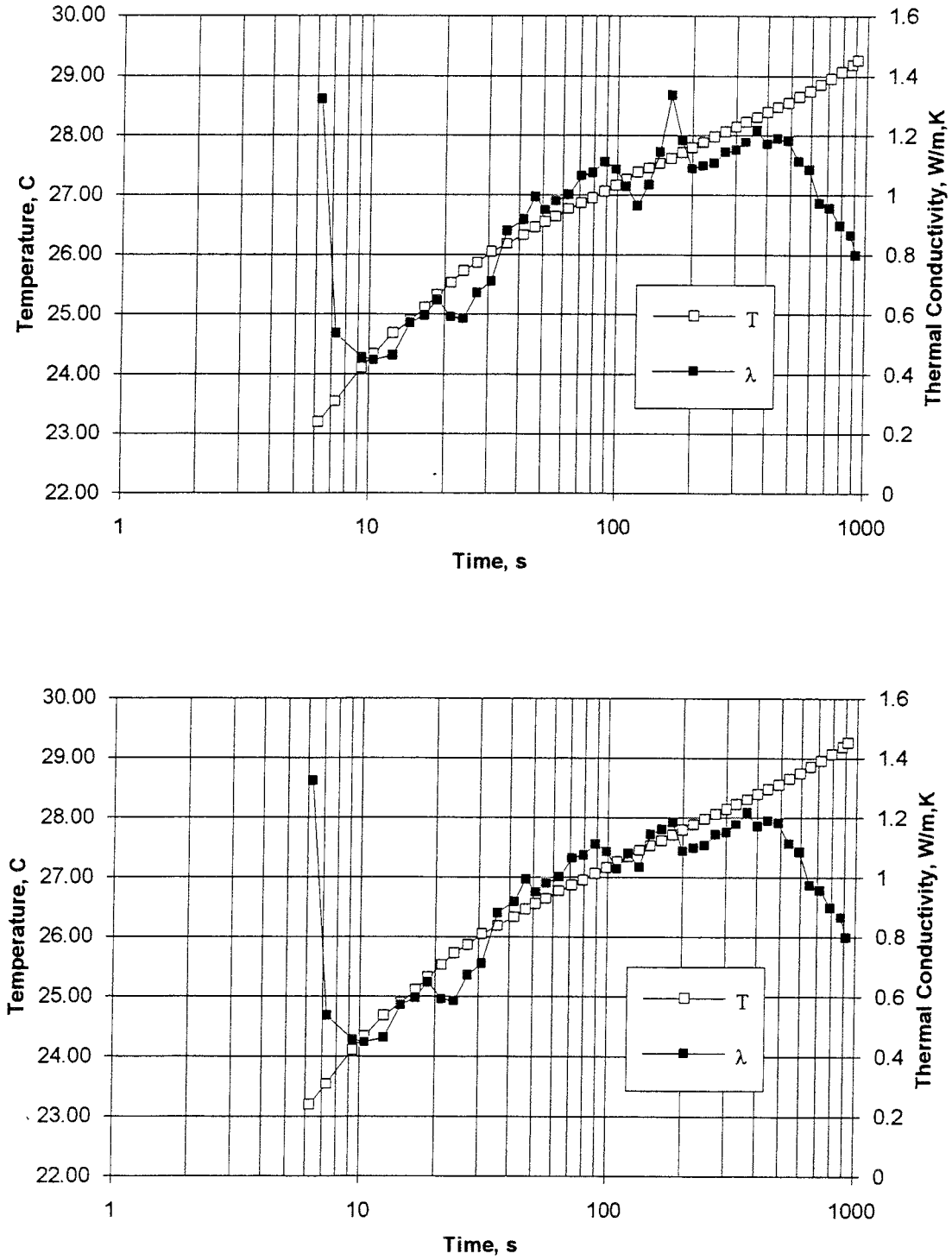

Figure 3-3 Thermal conductivity λ evaluated from average time and temperature values in short time intervals (upper diagram) and thermal conductivity with one temperature value changed from 27.38 °C to 27.35 °C (lower diagram)

4 CALCULATION OF THE INFLUENCE OF THE MEASURING TECHNIQUE

4.1 GENERAL

The experiments for determining the heat conductivity of buffer and backfill material with the thermal probe method have been modelled and calculated using FLAC, which is a two-dimensional explicit finite difference code for PC. Such calculations were justified by the need for improving the understanding of this experiment and for investigating possible limitations of the experiment concerning the following factors:

Geometry
Applied power
Available time limit
Heat transfer resistance between the probe and the sample
Effect of insulation at the axial and radial boundaries

The aim of these calculations was to develop the most appropriate test and evaluation method.

In most calculations an axi-symmetrical element model with a symmetry plane through the centre of the probe as shown in Fig 4-1 has been used. Table 4-1 shows the standard geometry, properties, and boundary conditions that have been used if nothing else is noted.

Table 4-1. Material indata for the calculations. The inner radius of the probe is 0.75 mm.

Material	Radial thickness mm	λ W/m,K	C_p Ws/kg,K	ρ kg/m^3	α W/m^2,K
Probe	0.75	14	460	7800	
Transition zone	0.75	0.2	2000	100	
Sample	22.75	1.2	1600	2000	
Insulation	20	0.036	2000	20	10

The results are given in the same type of diagrams as the laboratory tests, i.e. the calculated temperature and heat conductivity are reported as a function of the elapsed time. The heat conductivity is calculated for each pair of temperature values according to Eqn 3-5. Since the actual heat conductivity of the sample is known (indata parameter), the influence of different factors can be evaluated.

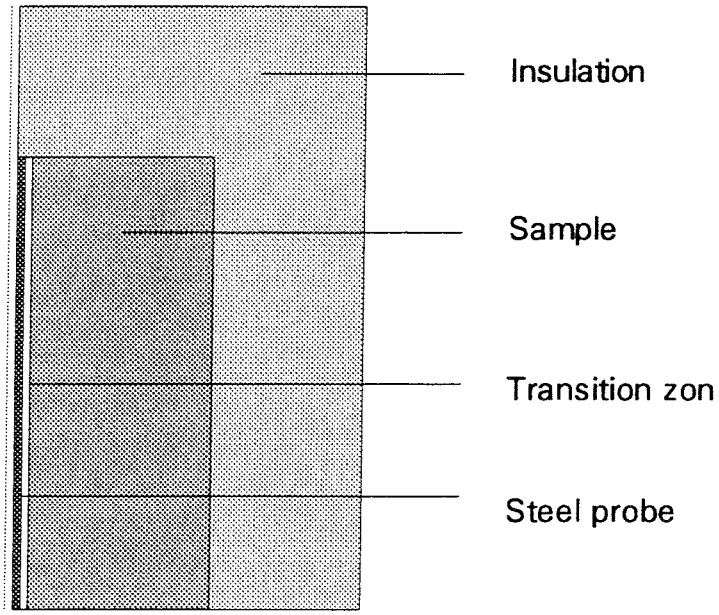

Figure 4-1 Geometrical model used for the FLAC calculations of the probe tests. The left boundary is rotational symmetric and the lower boundary is a symmetry plane.

4.2 INFLUENCE OF THE TRANSITION ZONE BETWEEN THE PROBE AND THE BENTONITE

As shown in Table 4-1, the heat resistance at the probe/bentonite contact was simulated by a 0.75 mm thick material, but the first simulation was made without introducing any contact resistance. Fig 4-2 shows the results from this calculation. They can be grouped referring to three periods. In the first period, i.e. the initial 30 seconds, the calculated heat conductivity is higher than the applied value λ=1.2 W/m,K. For the second, i.e. the period ranging from 30 and 300 seconds, the agreement is very good, while for longer periods of time than 300 s, λ is too low. The initial high value is caused by the influence of the probe material and the low value in the late part of the test is caused by the influence of insulation. With the applied geometry and materials there is obviously a period between 30 and 300 seconds that is suitable for evaluation of the heat conductivity. However, the low values that are measured at the end of the first and at the beginning of the second period are not obtained in the calculations and it is logical to believe that they are caused by the heat resistance of the transition zone.

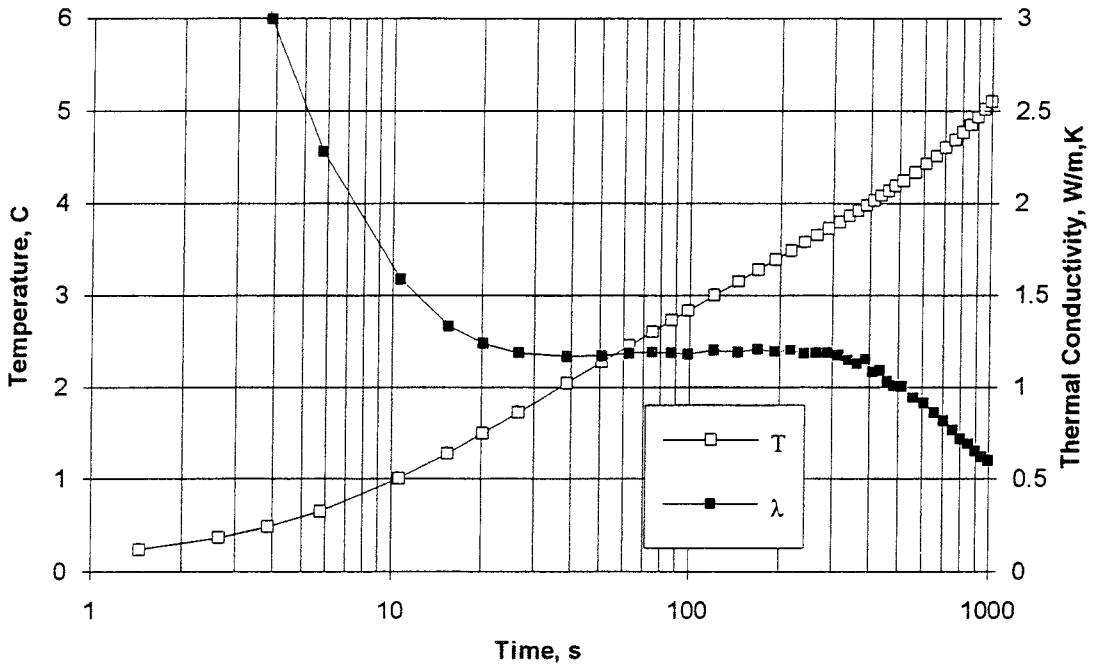

Fig 4-2 Temperature and thermal conductivity calculated from a FLAC simulation of a probe test with no heat resistance between the probe and the sample.

The thickness and thermal data of the transition zone were chosen to avoid numerical problems in the FLAC calculation. A number of calculations with different thermal resistance of the zone were made with the thermal conductivity varying between 0.02 W/m,K$\leq\lambda\leq$0.3 W/m,K, and the results of these calculations are shown in Fig 4-3. The figure clearly illustrates the influence of the transition zone. At a too high heat resistance (thermal conductivity of the transition zone less than 0.1 W/m,K) the influence will be so large that the heat conductivity of the sample is underestimated. This is because the evaluated λ-value is influenced by the insulation before it reaches its true value. By comparing Fig 4-3 and Fig 3-4 one finds that the heat resistance of the bentonite/probe contact in the laboratory test corresponds to the thermal properties of the contact zone in the calculation with $\lambda\approx$0.2 W/m,K. The dip in λ-value to $\lambda\approx$0.5 W/m,K at 10 seconds and the slow increase to a steady value after 100-200 seconds, as well as the temperature increase of about 8°C at 1000 seconds, are the same in the calculation and in the laboratory test. The calculation also indicates that a thermal resistance that yields a temperature increase by more than 10°C is not appropriate when the thermal conductivity of the sample is 1.2 W/m,K.

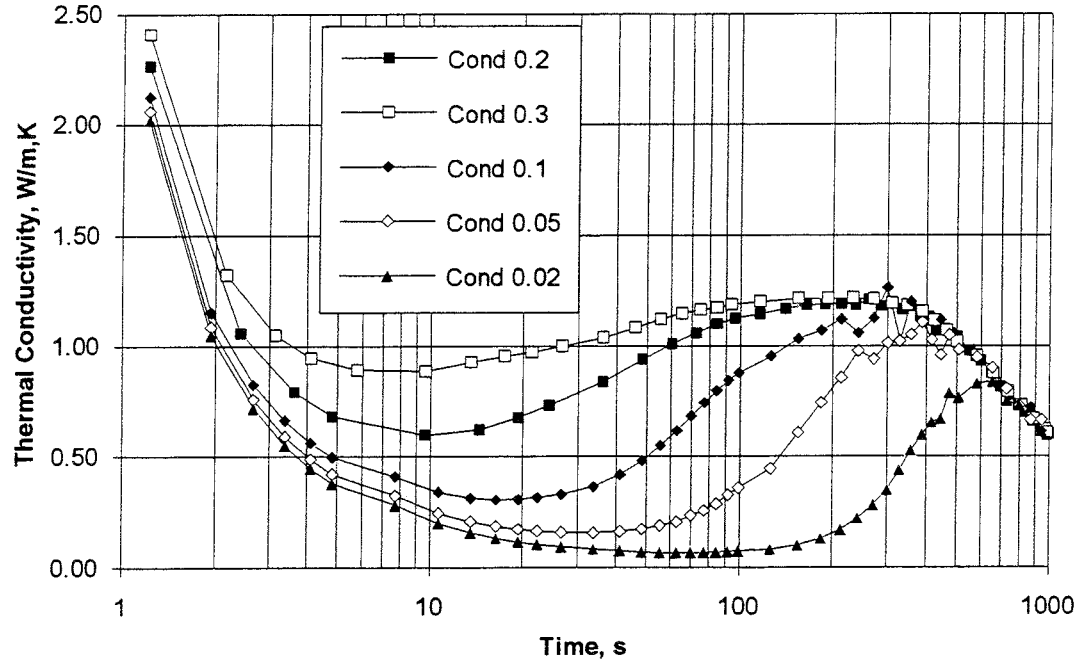

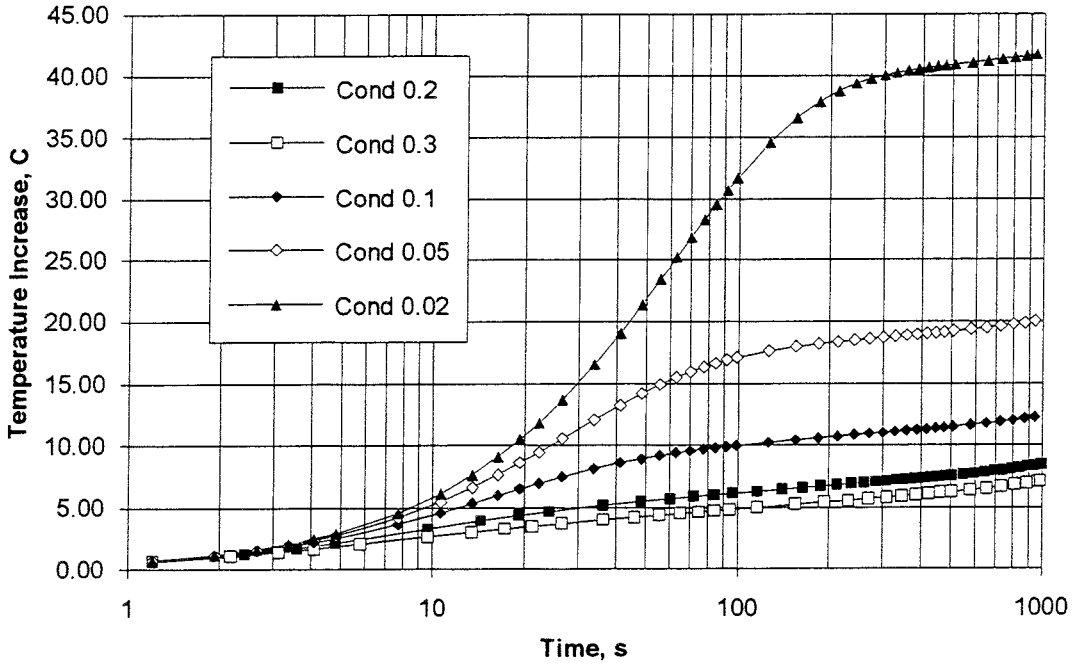

Fig 4-3 Temperature and thermal conductivity of a sample calculated from FLAC simulations of a probe test with different thermal properties of the transition zone between the probe and the sample.

4.3 INFLUENCE OF THE MATERIAL AND DIMENSIONS OF THE PROBE

The following two probe types were used in the laboratory tests:

- Probe made of corundum with the radius 5 mm
- Probe made of stainless steel with the radius 3 mm.

Fig 4-4 shows the results of two calculations with these two probes. The indata shown in Table 4-1 were used except for the corundum probe, for which the following values were given:

Corundum probe: λ=2.0 W/m,K; C_p=800 Ws/kg,K; ρ=2000 kg/m^3.

The corundum probe was simulated as a tube with an inner radius of 0.5 mm and an outer radius of 2.5 mm. The radial thickness of the sample was accordingly smaller (21.75 mm). The results show that there is a considerable difference in evaluated heat conductivity in the beginning of the test but that there is no difference for t>100 seconds. The conclusion is thus that both probes are suitable and yield the same results.

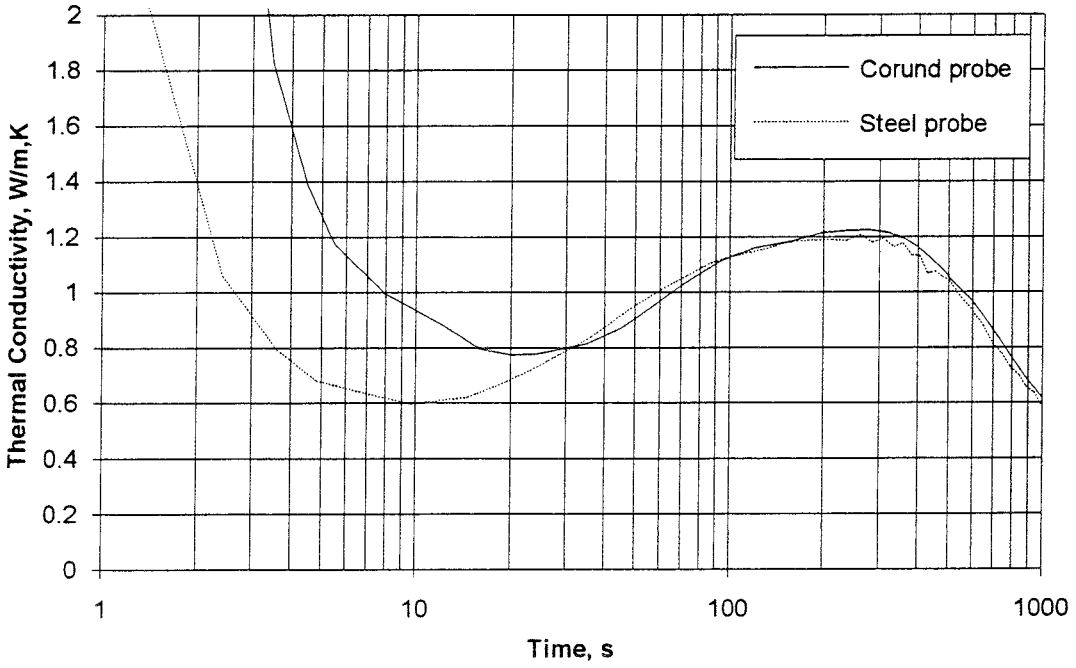

Fig 4-4 Comparison of the evaluated thermal conductivity of a simulated test on a clay sample from FLAC calculations with a steel and a corundum probe. The actural thermal conductivity of the clay sample was 1.20 W/m,K

4.4 INFLUENCE OF THE HEAT CONDUCTIVITY OF THE SAMPLE

The influence of the heat conductivity on the results was investigated by comparing two identical calculations with different indata for the sample. The old calculation with λ=1.2 W/m,K and a new one with λ=3.0 W/m,K are compared in Fig 4-5. The figure shows that the calculated heat conductivity does not reach the indata value when the sample radius is 2.5 cm and the heat conductivity is as high as λ=3.0 W/m,K. The sample is too small since the heating front hits the boundary much earlier than in the other calculations. A larger sample is thus required as shown in chapter 4.6.

4.5 INFLUENCE OF APPLIED POWER

The influence of power applied to the probe is illustrated in Fig 4-6, showing the results of two calculations with the probe powers 1 W and 4 W. The diagrams show that although the temperature increase is much higher for the calculation with the high power, the evaluated heat conductivity is an almost identical function of time. This shows that a change in power does not affect the accuracy of the evaluated thermal conductivity and a reduction in power is hence of no help if the sample is too small. As mentioned earlier, a high power may yield too high temperatures with undesired vapor flux.

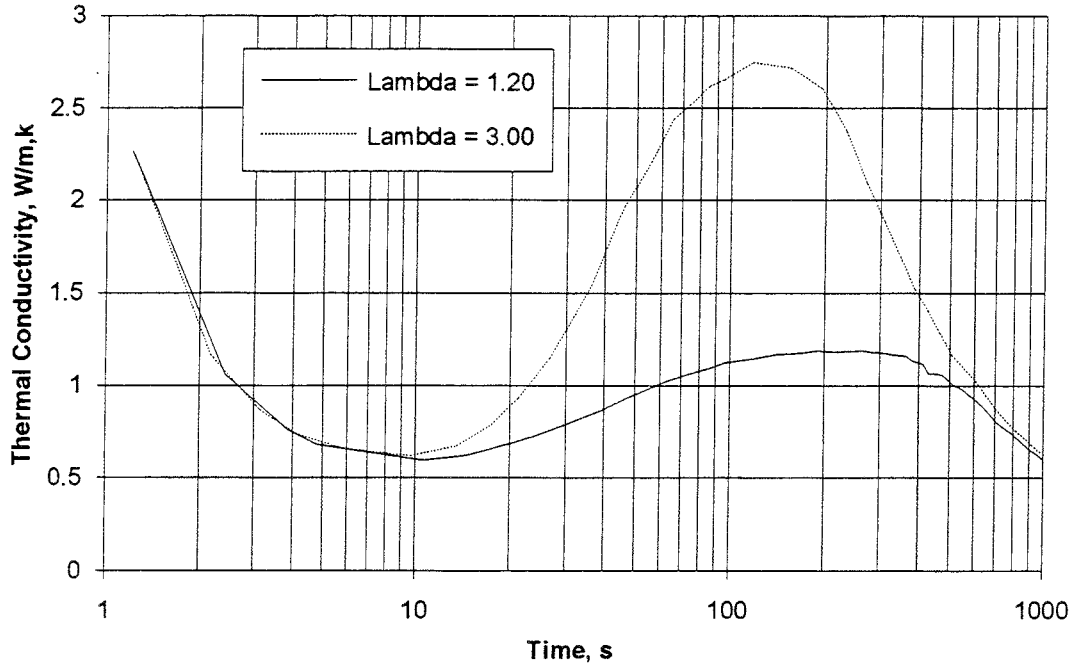

Fig 4-5 Influence of the thermal conductivity of the sample. FLAC calculations of two probe tests on two samples with quite different thermal conductivity.

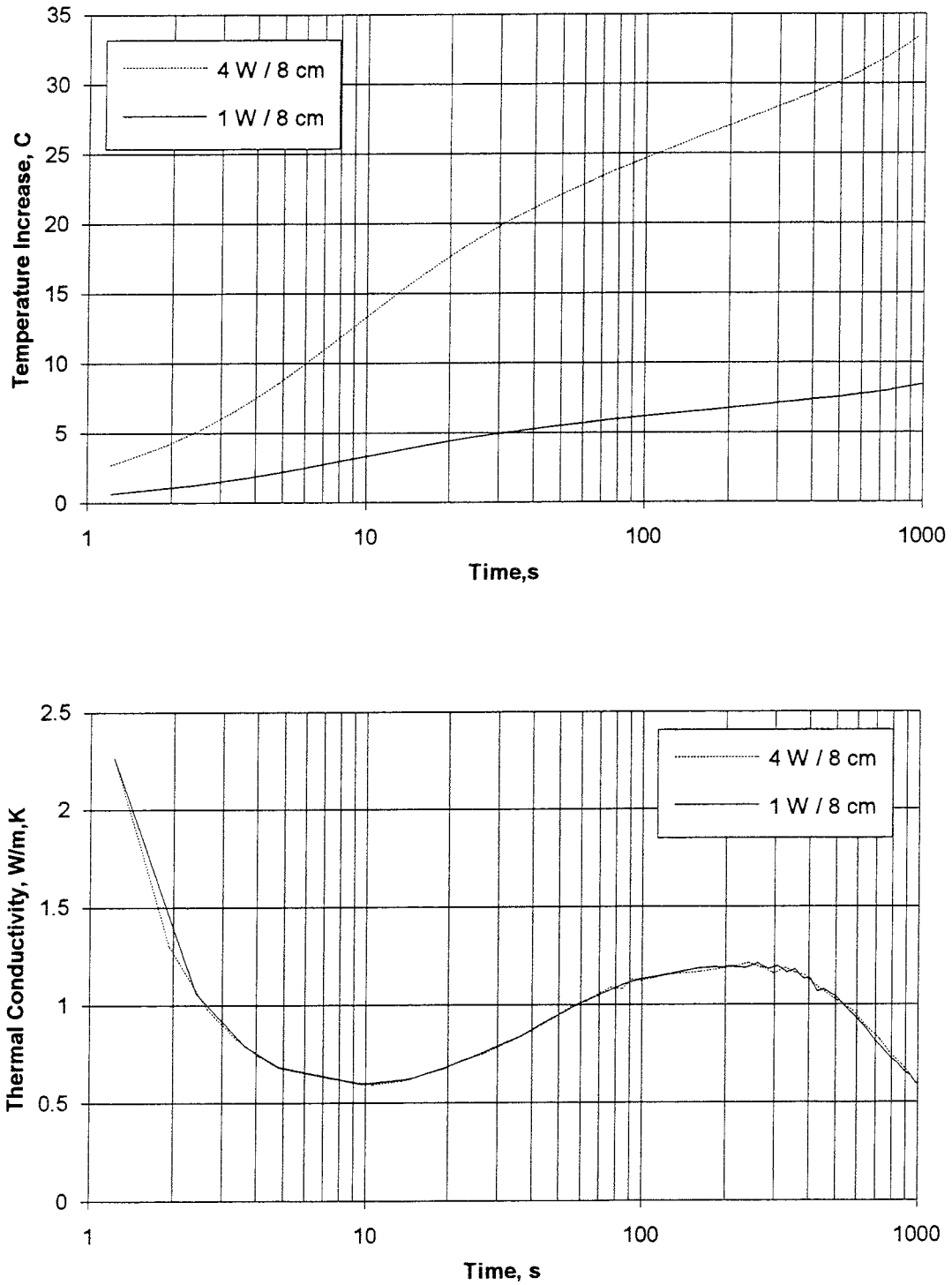

Fig 4-6 Influence of the applied power. FLAC calculation of two probe tests with different applied probe power.

4.6 INFLUENCE OF SAMPLE GEOMETRY AND PROBE LOCATION

In order to investigate the influence of the radial size of the sample the same calculation as shown in chapter 4.4 was made but with the radius 5.0 cm of the sample instead of 2.5 cm. Fig 4-7 shows the results of both calculations with λ=3.0 W/m,K as indata for the sample. The calculated thermal conductivity of the large sample yields λ=3.0 W/m,K for the time period 250-500 seconds while λ for the small sample never reached the correct value. A sample with at least 5 cm radius is thus required when the heat conductivity is that high.

Most measurements have been made with a probe that has the same length as the axial length of the sample and with insulation at the end faces (see Fig 3-1). Since it is interesting to see if the probe can be used by directly inserting it in a large block before it is installed in a repository, and to find out if the probe can be used to measure the heat conductivity during water uptake in a test site, a calculation was made for the case of a probe penetrating a 20 cm thick clay block with large lateral extension. Fig 4-8 shows the results of a calculation were the probe is 8 cm long and the sample 8 cm in radius and 20 cm long, which means that the probe is completely embedded in the clay. The results are compared with the results of the standard calculation. It is obvious that it is much more difficult to evaluate that kind of test since the calculated heat conductivity increases with time and there is no time after which the result becomes erroneous. The axial heat transport is too large after about 200 seconds. It seems thus that the length/diameter relation needs to be larger than 25 to yield good results if this type of test is made.

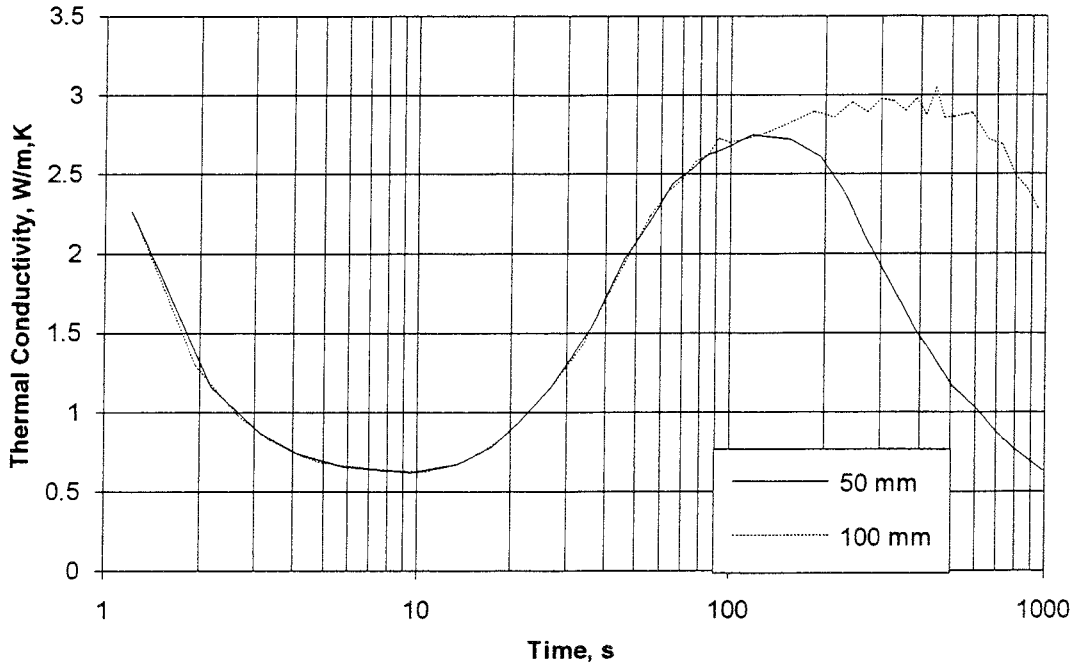

Fig 4-7 Influence of the diameter of the sample on the evaluated thermal conductivity. FLAC calculations of two probe tests on samples with the thermal conductivity 3.0 W/m,K.

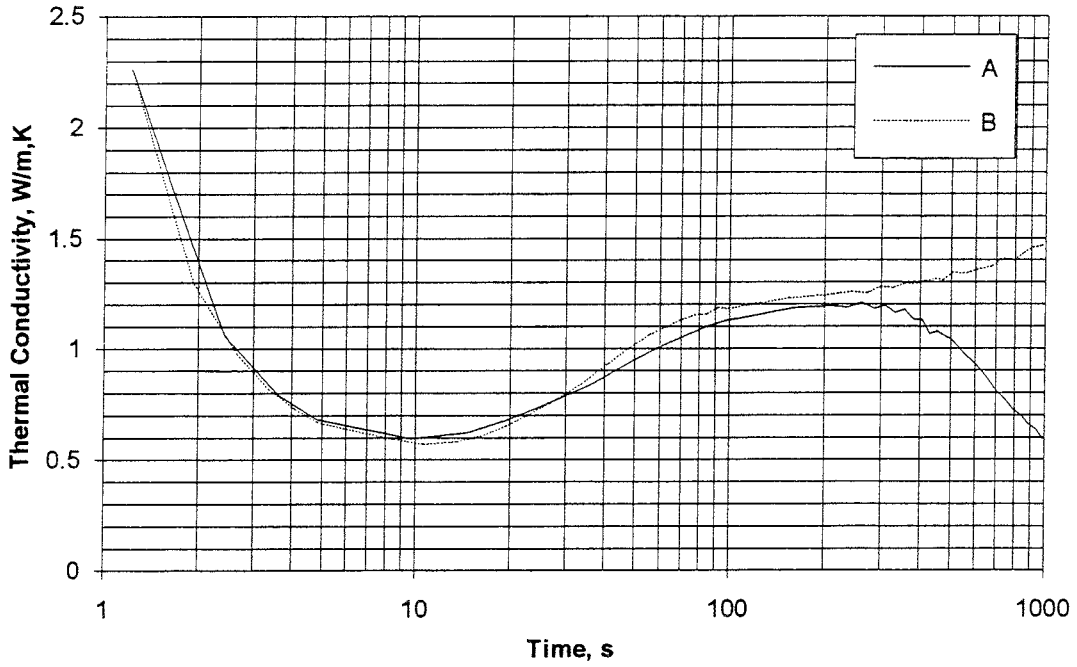

Fig 4-8 Evaluated thermal conductivity from a FLAC calculation of a probe test on a probe embedded in a large clay sample (B), compared with the standard method (A)

The influence of the probe length when it is embedded in the clay is shown in Fig 4-9, where two calculations with the probe lengths 8 and 10 cm are compared. The influence of extending the probe by 25% from 8 cm to 10 cm clearly improves the result. If the difference is extrapolated, it is found that a probe length of about 15 cm is enough to yield acceptable results. This means that the length/diameter relation should be about 50. However, further investigation is needed before this principle can be applied.

4.7 INFLUENCE OF SAMPLE INSULATION

The end faces do not need to be insulated, which is shown by the comparing FLAC calculations in Fig 4-10. The reason is that the axial heat loss is very small with the applied heat transfer coefficient α=10 W/m^2,K. However, the real value of α is not known and all tests have, for safetey reasons, been made with axial insulation.

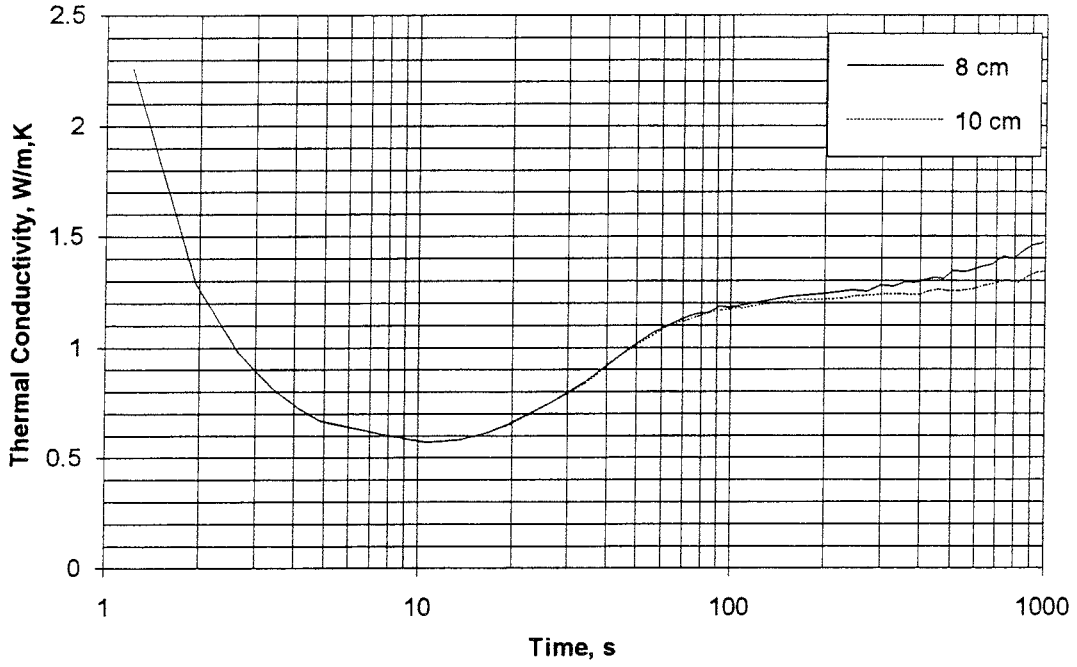

Fig 4-9 Influence of probe length. Evaluated thermal conductivity from two FLAC calculation of probe tests with different probe length. The probes are embedded in large clay samples.

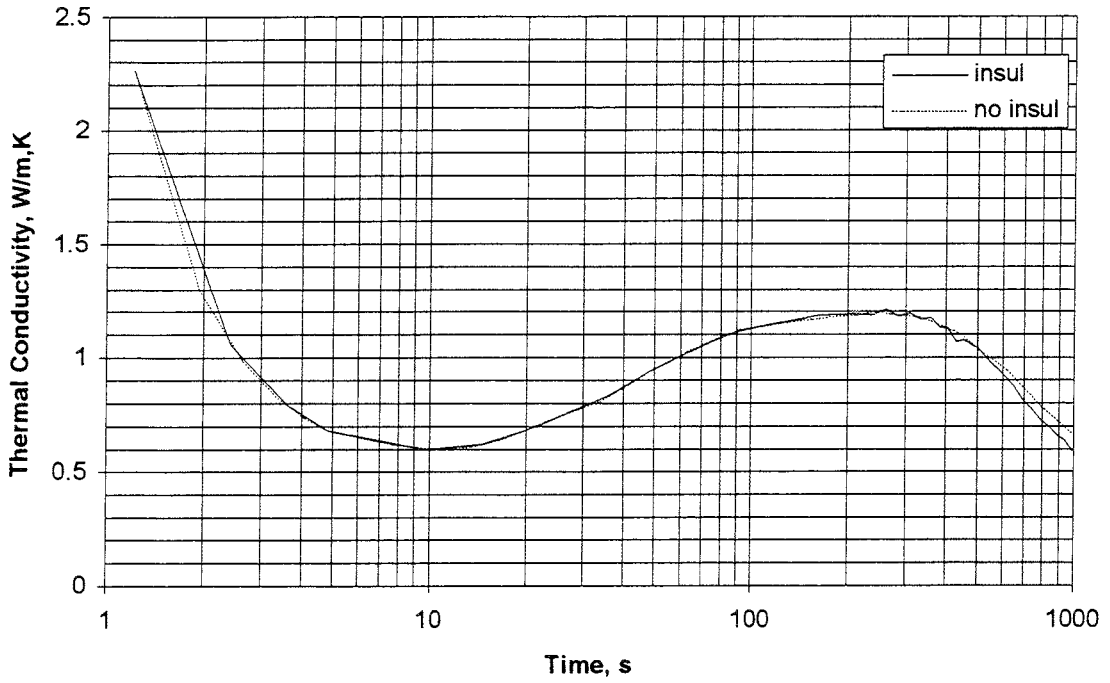

Fig 4-10 Influence of insulation at the sample boundaries. FLAC calculations of probe tests with insulated and not insulated samples.

4.8 INFLUENCE OF HEAT LOSS THROUGH THE PROBE CABLES

The axial heat transport is enhanced by the cables leading through the insulation to the top of the probe. The effect of this was investigated through a calculation in which the copper in the cable through the insulation was simulated as a conductor. In order to avoid numerical problems, the diameter of the copper was taken to be the same as the diameter of the probe, and the heat conductivity of the copper was reduced in proportion to the increased area. The cable was simulated to extend 10 cm outside the insulation. The results, which are given in Fig 4-11, showed that the influence of heat loss through the cables is very small.

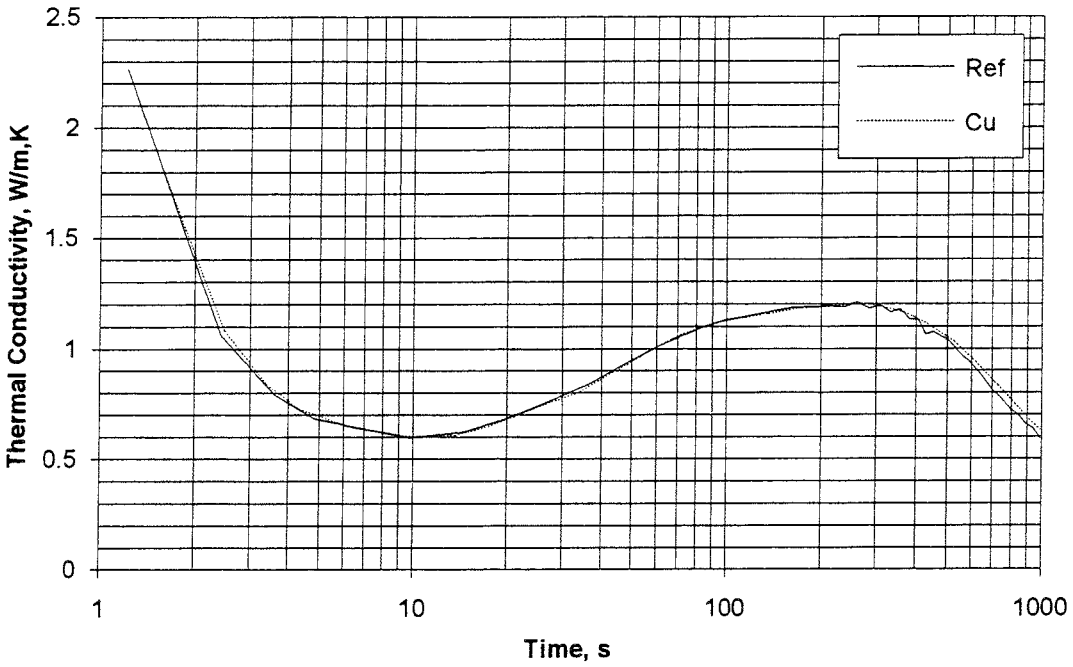

Fig 4-11 Influence of the probe cables on the evaluated thermal conductivity. Cu denotes the FLAC simulation with copper cables and ref denotes the reference FLAC simulation.

5 RECOMMENDED TEST AND EVALUATION METHODS FOR HEAT CONDUCTIVITY MEASUREMENTS

The test calculations using FLAC, and some preliminary experiments, have yielded a good understanding of the limits and critical parameters of heat conductivity testing applying the probe method. They have formed the basis of the following recommended standard method which has been used in most measurements:

Probe

A probe of stainless steel with 3 mm diameter and 80 mm length served as a standard tool in all tests on laboratory-compacted clays. Stainless steel is the recommended material but the length and diameter may of course be different, and the length/diameter ratio, which is 27 for this probe, can probably be lower if the sample has the same length as the probe and the end faces are insulated. However, a length/diameter ratio higher than 50 seems to be required if the sample is longer than the probe.

Sample

The standard diameter for the sample is 5 cm, which is sufficient if the heat conductivity of the sample is lower than about 1.5 W/m,K. The standard length of the sample is 8 cm and it is most important that the sample has the same length as the probe if the length/diameter ratio of the probe is lower than 50.

If the heat conductivity of the sample is higher than 1.5 W/m,K, its diameter needs to be larger than 5 cm. 10 cm seems to be sufficient for a sample with λ=3.0 W/m,K.

Probe/sample contact

The thermal resistance between the probe and the sample should be as low as possible. This can be achieved by drilling a hole in the sample with the same diameter as the probe and by applying heat paste (silicon grease) on the probe before installation. The thermal resistance of the contact zone can be checked by use of the recorded temperature increase of the probe. It should not exceed about 10°C when the heat conductivity of the sample is $\lambda \approx 1.2$ W/m,K and 15°C at $\lambda \approx 0.6$ W/m,K. These figures refer to the applied power of about 1 W per 10 cm probe length.

Insulation

Although the calculations showed that the insulation has only little influence on the results due to the small heat loss between the sample and the

surrounding air, it is recommended to use radial as well as axial insulation, since the actual heat transfer to the air is not well known.

Probe power

Theoretically, the applied power does not influence the evaluation. However, it needs to be sufficiently high to yield temperatures that can be measured with high accuracy, but not high enough to produce a temperature gradient that causes moisture redistribution in the sample. The power 1 W in the 8 cm long probe has been chosen as standard value, since it seems to be acceptable both concerning measurement accuracy and moisture redistribution. However, no investigation has been made to find out for what power the moisture redistribution becomes unacceptable.

Evaluation of λ

The temperature measurements should be made with short intervals, preferably about one per second. The average temperature within the sample should be calculated for constant intervals on a logarithmic time scale and plotted as shown in Fig 3-4. The heat conductivity can then be obtained by using Eqn 3-5, with the relation $\ln(t_2/t_1)/\Delta T$ graphically evaluated by drawing the best fitted straight line for the respective time interval between the parts influenced by the probe/sample resistance and the boundary. This time interval is usually $100s<t<400s$ and it is often easy to find the proper interval if the λ *vs logt* curve is evaluated and plotted as shown in chapter 3.4.

6 RESULTS FROM LABORATORY MEASUREMENTS OF HEAT CONDUCTIVITY

6.1 GENERAL

Several series of heat conductivity tests have been made for different purposes. The following test series will be accounted for:

- Measurements on water saturated samples with different void ratios. Purpose: to find the influence of the void ratio.
- Measurements on samples with the same void ratio but different degree of water saturation. Purpose: to find the influence of the degree of saturation.
- Measurements on sand/bentonite mixtures. Purpose: to find the influence of adding quartz sand to the bentonite.
- Measurements on blocks used for the Buffer Mass Test in Stripa. Purpose: to re-evaluate the BMT results.
- Measurements to investigate the influence of probe design

6.2 HEAT CONDUCTIVITY OF WATER SATURATED SAMPLES

Water saturated samples were taken either from test samples used in triaxial tests, with saturation before the triaxial tests, or directly from samples saturated in the so-called saturation apparatus. It is shown in Fig 6-1. The sample is made of 5 compacted unsaturated samples with height 20 mm and diameter 50 mm piled inside the apparatus. The chamber is confined and deaired by vacuum suction and water is let into the chamber and the filters. A backpressure of 500 kPa was also applied to the water in order to increase the saturation rate. However, the samples did not reach complete saturation, partly because they expanded elastically when taken out from the apparatus. Only two samples were made in this fashion.

The results of the measurements are shown in Table 6-1.

Table 6-1. Compilation of measurements made on samples close to water saturation. The note *satap* means that the samples were prepared in the saturation apparatus. The other samples were taken from triaxial tests.

Bentonite type	e	S_r %	λ W/m,K	Note
SPV 200	1.4	99	1.10	
IBECO-Na	1.5	98	1.14	
Mx-80	1.4	98	1.10	
Mx-80	1.33	100	1.24	
Mx-80	1.23	98	1.26	
Mx-80	0.64	92	1.24	satap
Mx-80	0.81	97	1.28	satap

These results are analysed in chapter 8.

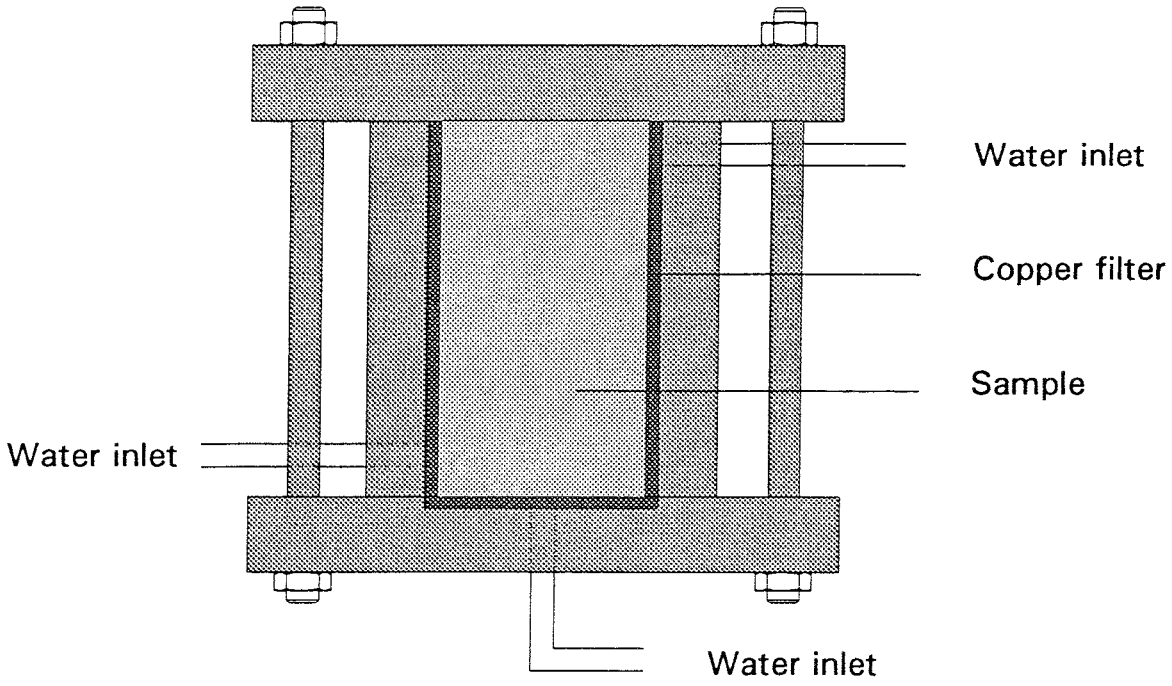

Fig 6-1 Saturation apparatus

6.3 DETERMINATION OF THE INFLUENCE OF THE DEGREE OF WATER SATURATION ON THE HEAT CONDUCTIVITY

A series of tests were made on samples with the void ratio e=0.8 and with water ratios varying between that of air-dry bentonite, i.e. w=10% and w=25%, which corresponds to almost complete saturation. The purpose was to investigate the influence of the degree of water saturation on the heat conductivity, which is important for understanding the effect of drying and water redistribution on the temperature in a repository.

The samples were compacted to blocks with the dimensions 200x100x75 mm^3. Different degrees of saturation were obtained by adding different amounts of water to the bentonite before compaction. The void ratio e=0.8 was achieved by compacting the blocks to a defined height. The actual void ratios were a little higher than the intended one due to lack of precision during compaction and because the swelling was different at different degree of saturation.

The blocks were cut in two equally large pieces (100x100x75 mm^3) which were both used for heat conductivity testing. One part was tested the same day as compaction had been made, while the other was wrapped in plastic and stored for about 4 weeks before testing. The water ratio and density determinations, which were made after the testing, showed that the two halves were not completely equal. The stored sample had dried somewhat and shrunk by a few per cent. The results of these tests are shown in Table 6-2, which also includes one of the tests from Table 6-1.

Table 6-2 Compilation of all tests on samples with void ratio close to e=0.8

Block No	ρ, t/m^3	w, %	e	S_r, %	λ, W/m,K
1	1.90	25.2	0.83	85	1.21
2	1.84	21.9	0.83	73	1.15
3	1.78	18.1	0.85	59	0.93
4	1.72	15.4	0.87	49	0.79
5	1.69	14.3	0.88	45	0.72
1	1.90	24.0	0.81	82	1.23
2	1.85	20.7	0.82	70	0.90
3	1.78	17.4	0.84	58	0.88
4	1.72	14.5	0.85	47	0.70
5	1.69	13.2	0.86	43	0.61
6	1.97	28.4	0.81	97	1.28

The evaluated thermal conductivity is plotted as a function of the degree of saturation in Fig 6-2. The diagram shows that the values form a fairly distinct line with quite small scatter in spite of the difference in void ratio, except for the sample with S_r=70%. The diagram also shows that the influence of the degree of saturation is larger in the interval 40%<S_r<60% than when the degree of saturation exceeds S_r>80%. However, the error obtained if the relation is approximated to a straight line is not very large.

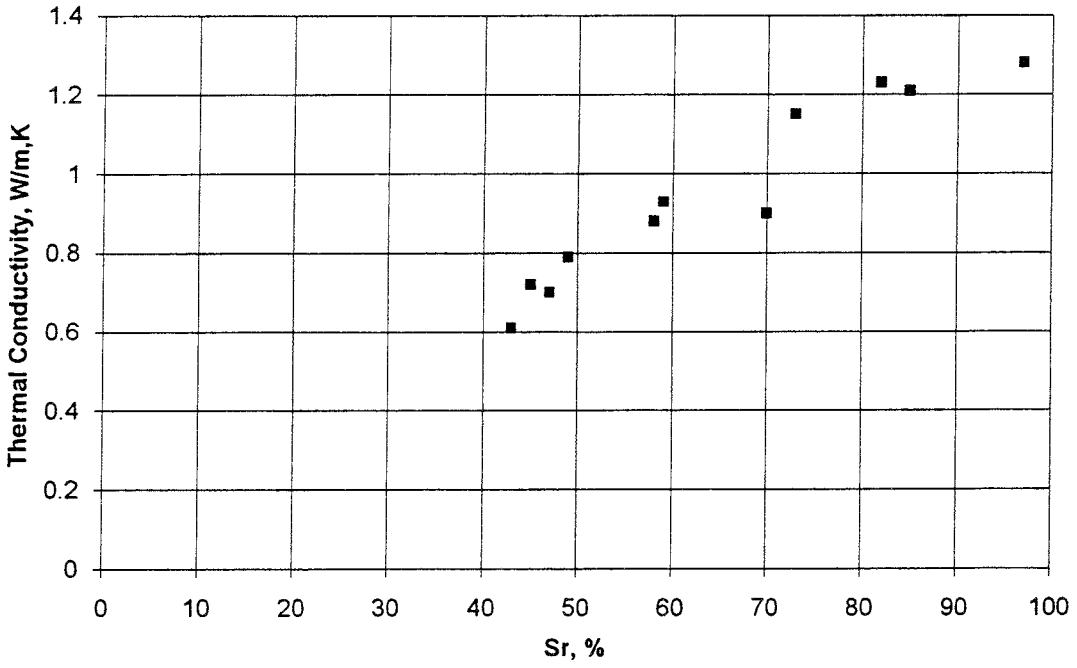

Fig 6-2 Thermal conductivity measured on samples of Mx-80 with void ratio $e \approx 0.8$ plotted as a function of the degree of water saturation

6.4 SAND/BENTONITE MIXTURES

Two measurements on sand/bentonite mixtures have been made on samples extracted after triaxial testing. The results are shown in Table 6-3.

Tabell 6-3 Thermal conductivity of mixtures of bentonite SPV200 and quartz sand

Mixture	e	Sr %	λ W/m,K
SPV/Sand 50 % / 50 %	0.45	95	1.78
SPV/Sand 30 % / 70 %	0.39	93	2.51

The tests show that the thermal conductivity is considerably higher than for 100% bentonite, as expected.

6.5 BLOCKS USED FOR THE BUFFER MASS TEST IN STRIPA

In order to evaluate the difference between heat conductivity values derived from laboratory tests, and data evaluated from field tests, measurements were made on dense blocks of the same type as used in the Stripa Buffer Mass Test. The blocks were investigated for different e and S_r, referring to

different stages of the field test. The results are shown in Table 6-4. Two measurements were made on two of the blocks (λ_1 and λ_2).

Tabell 6-4 Thermal conductivity of some blocks of Mx-80

Block type	e	Sr %	λ_1 W/m,K	λ_2 W/m,K	λ_{av} W/m,K
1	0.44	55	1.04	0.95	1.00
2	0.65	57	1.03	1.10	1.06
3	0.64	92	1.24		1.24

Block types:

1. Block compacted for BMT in Stripa
2. Block compacted in the way described in chapter 6.3
3. Block made and saturated in the saturation apparatus

These results will be discussed in chapter 8.

6.6 INFLUENCE OF THE PROBE TYPE

Five measurements with each of the two probe types (corundum and steel) were made in conjunction with earlier tests on graphite mixed bentonite. The purpose of mixing graphite with the bentonite was to increase the thermal conductivity. IBECO bentonite was used for these tests. The results are shown in Table 6-5.

Table 6-5 Comparison of heat conductivity measured with two different probes

Graphite content	Sr	*e*	λ, steel	λ, corundum	Note
%	%		W/m,K	W/m,K	
10	29		0.60	0.63	
5	37		0.71	0.71	
10	98		3.07	3.15	
20	96		3.11	3.15	
20	33		1.34	1.09	1

Note 1: Poor contact between probe and sample when the corundum probe was used (too high heat resistance)

The results confirm the conclusion from the calculations that both types are suitable and give similar results although the poor contact invalidated the results in the last test with the corundum probe.

7 HEAT CONDUCTIVITY EVALUATED FROM BACK-CALCULATIONS OF FIELD TESTS

7.1 GENERAL

The following three field tests made in the Stripa mine will be investigated:

- The buffer mass test (BMT)
- The settlement test
- SKB/CEA test of French clay

The two former tests were made with Mx-80 bentonite and the latter test made with the French reference buffer material Fo-Ca. Proper back-calculation of the heat conductivity requires accurate results from temperature calculations that take into account the properties and geometry of the system. The SKB/CEA test had a geometry that makes the back-calculations fairly simple, and the settlement test was accurately back-calculated after the test, while the BMT test needs to be recalculated since the old evaluation was a prediction that didn't take all circumstances during the test into account.

7.2 TEMPERATURE CALCULATION OF THE BUFFER MASS TEST

The Buffer Mass Test in Stripa was a simulation at half scale (diameter) of 6 deposition holes. The simulated canisters were heated to temperatures that did not exceed 90°, except for hole 2 in which the temperature of the canister after 2.4 years was increased to 138°C during 0.9 years. The tests were terminated and the buffer material excavated after 0.9 to 3.3 years. These tests are valuable for back-calculating the in-situ heat conductivity of the buffer material.

The calculation for BMT was made with the finite element program Microfield. The transient temperature increase due to a power of 600W applied to the heater was calculated for up to 3.5 years. The element mesh was rotational symmetric around the central axis of the heater and the mesh made of 17x32 elements with the distance 25 m to the radial boundary and 15 m to the axial boundary, which was far enough to exclude the influence of the boundary conditions. The element mesh is shown in Fig 7-1 and the thermal properties of all materials are collected in Table 7-1.

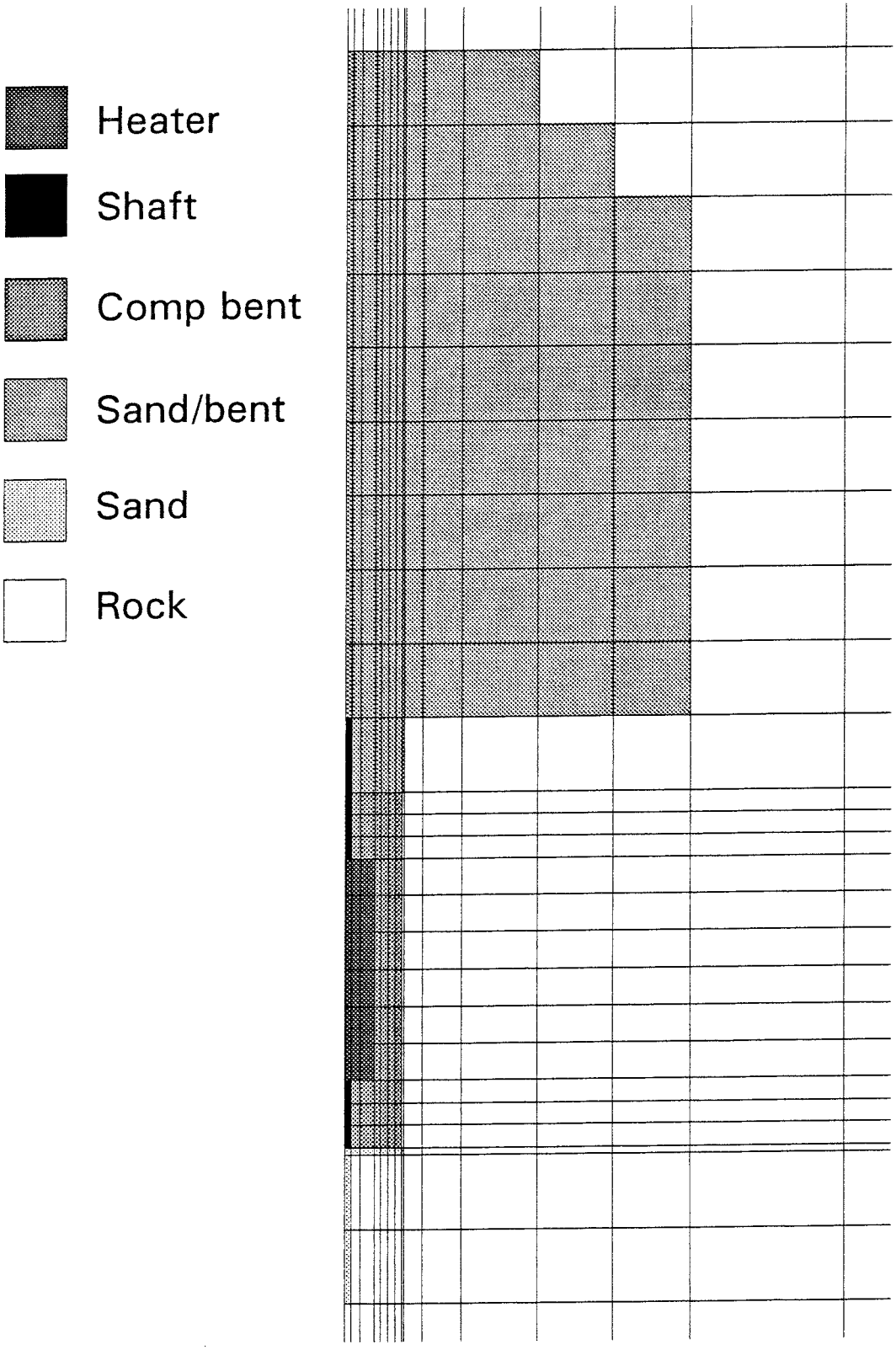

Figure 7-1 Element mesh and materials with different thermal properties used in the finite element calculation of the Buffer Mass Test

Table 7-1 Thermal indata for the BMT calculation.

Material	λ W/m,K	C_p Ws/kg,K	ρ kg/m^3
Heater	59	460	7800
Heater shaft	14.75	460	7800
Buffer	1.0-1.45	1100	2170
Backfill	2.2	1400	2150
Sand	2.1	1600	2100
Rock	3.6	800	2700
Slot	0.5	4200	1000

The influence of the boundary conditions was investigated by comparing calculations with different boundaries. There was no difference between the results from the calculations after 3.5 years for the condition of no heat transfer, and for constant temperature at the boundaries. Some of the calculations included a slot with λ=0.5 W/m,K corresponding to the initial state with water in the slot between the bentonite blocks and the rock. The calculations used for evaluating the geometry effect had no slot since it referred to the average properties of the buffer.

The six deposition holes in the buffer mass test had slightly different geometries and buffer composition. The"wet holes" (1,2, and 5) had an empty slot of 1 cm while the "dry holes" (3,4 and 6) had a slot of 3 cm that was filled with uncompacted bentonite. Holes 1 and 2 had the entire overlying tunnel backfilled while only confined concrete boxes with the dimensions 1.8x1.8x1.5 m^3 were backfilled on top of the other holes.

The calculations referred to the conditions in holes 1 and 2. The influence of the other geometries was considered by comparing results from earlier calculations at different geometries. These calculations showed that the expected temperature drop across the central section of the buffer was 2.7% lower when boxes were used than in the case of a backfilled tunnel.

The following examples of results from the following three calculations will be given:

BMT7: Calculation simulating the conditions in the beginning of the test with a slot with λ=0.5 W/m,K and bentonite blocks with λ=1.0 W/m,K.
BMT8: Calculation simulating the condition at the end of the test with a water saturated homogeneous buffer with λ=1.35 W/m,K
BMT9: Do. with λ=1.45 W/m,K.

The calculated temperature distributions in the central section at different times are shown in Fig 7-2. These results will be used in chapter 7-3.

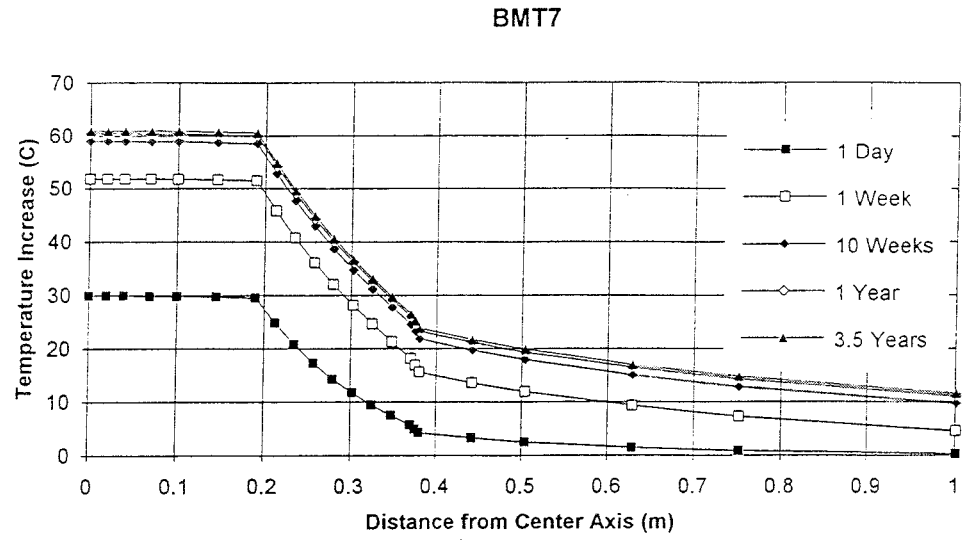

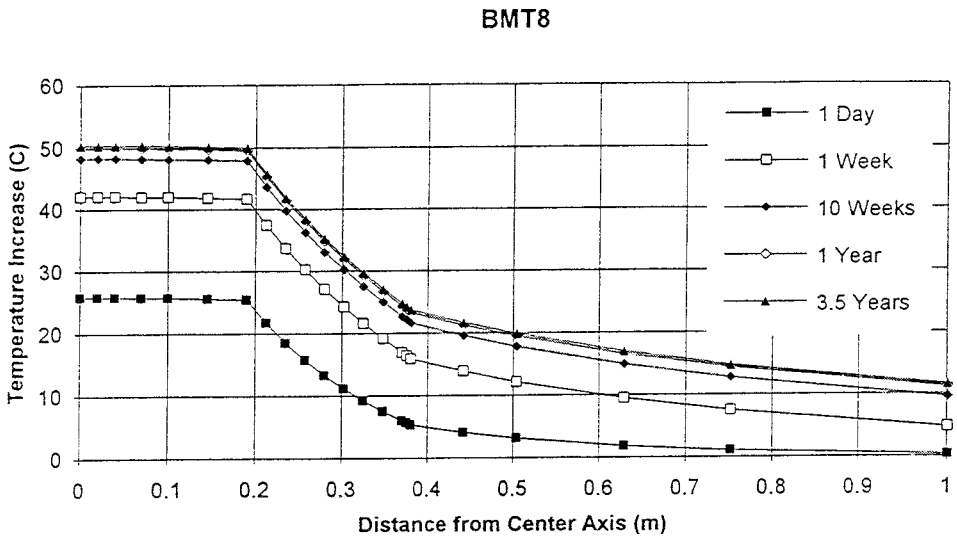

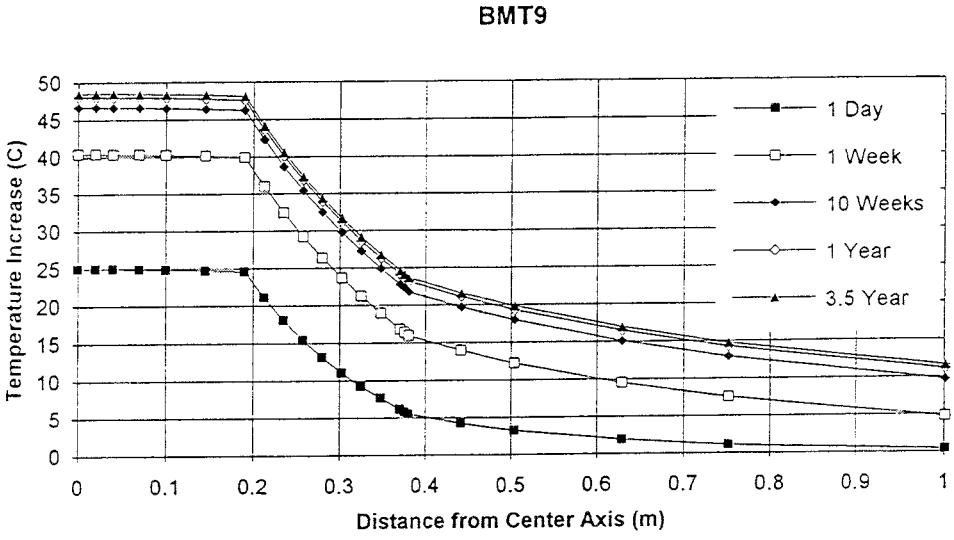

Figure 7-2 Calculated temperature distribution in the central section of the canister.
BMT7: Unsaturated blocks with λ=1.0 W/m,K and a slot at the rock.
BMT8: Saturated buffer with λ=1.35 W/m,K.
BMT9: Saturated buffer with λ=1.45 W/m,K.

7.3 HEAT CONDUCTIVITY EVALUATED FROM BMT

The back-calculation and evalution have been made in the following way:

For steady state conditions, the drop in temperature ΔT over an axial symmetric medium between the radius R_1 and R_2 can be calculated as a function of the centrally applied power P according to Eqn 7-1.

$$\Delta T = \frac{P/L \cdot ln(R_2/R_1)}{2\pi \cdot \lambda} \qquad (7\text{-}1)$$

where L is the length at which P is applied. This equation can be used to evaluate λ if the drop in temperature is known. However, Eqn 7-1 is valid for an infinitely long geometry which means that it is only valid if L/R_2 is large enough. In BMT, the length of the canister was 1.5 m, the outer radius corresponding to the radius of the hole was R_2 = 0.38 m and the inner radius corresponding to the radius of the canister was R_2 = 0.19 m. The geometry of holes 1 and 2 is shown in Fig. 7-3, which demonstrates that a steel shaft is attached to the canister at the upper end and a steel bar to its lower end. They increase the axial loss of heat.

A factor for correcting the axial loss of heat is thus needed and it can be taken from the results of the FEM calculations in chapter 7.2. According to these calculations a drop of 26.21°C in temperature between R_1 = 0.19 m and R_2 = 0.38 m after 3.5 years takes place for the geometry of holes 1 and 2 if λ = 1.35 W/m,K. Introducing these data in Eqn 7-1, one finds that λ = 1.68 W/m,K. The correction factor for achieving the correct value of λ is thus C = 1.25.

The same calculation for holes 3 to 6, which had small boxes above the holes, yields according to chapter 7.2 the correction factor
$C = 1.027 \cdot 1.25 = 1.28$

The heat conductivity of the entire buffer mass between the canister and the rock (including slots) can thus be calculated according to Eqn 7-2.

$$\lambda = \frac{P/L \cdot ln(R_2/R_1)}{2\pi \cdot \Delta T \cdot C} \qquad (7\text{-}2)$$

where C is the correction factor and ΔT is the measured temperature difference. C = 1.25 for holes 1 and 2 and C = 1.28 for holes 3-6.

The tests in all holes were evaluated according to Eqn 7-2 for different times after test start. Table 7-2 shows the results.

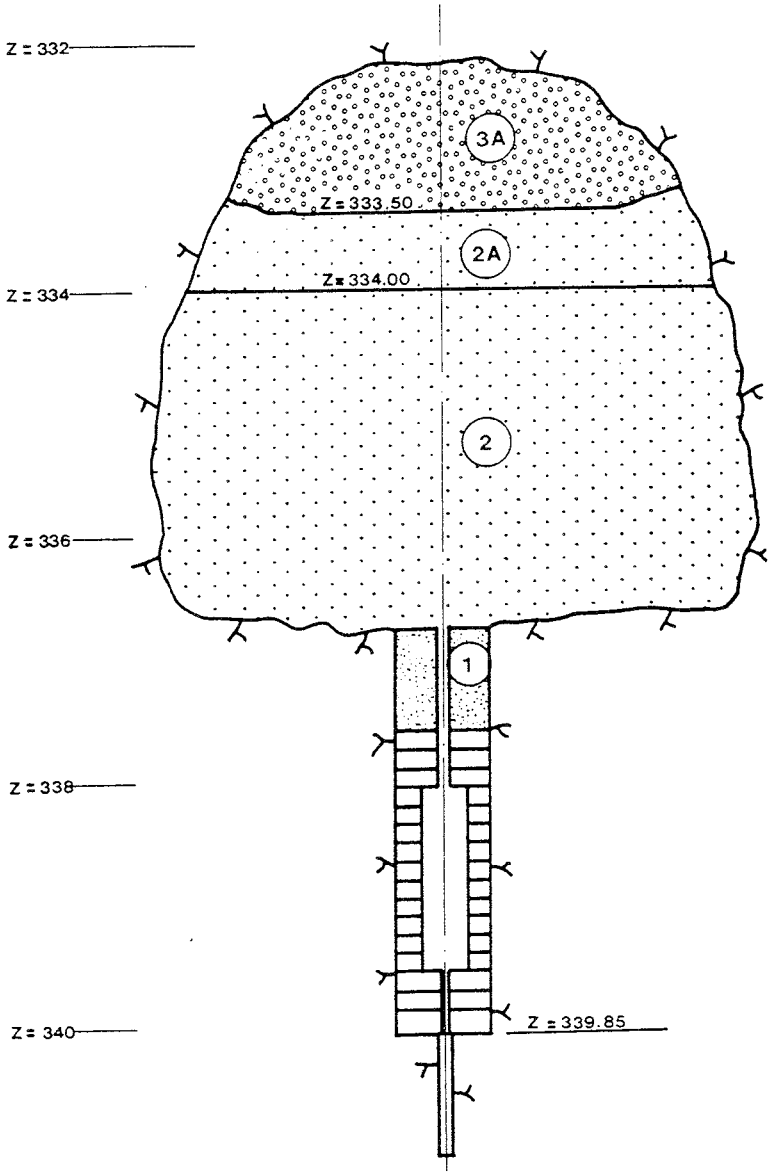

Figure 7-3 Cross section of holes 1 and 2 in BMT. 1, 2 and 2A denote 10/90 compacted bentonite/sand mixtures and 3A denotes 20/80 shotcreted bentonite/sand mixture

Table 7-2 Measured temperature drop ΔT (°C) between the canister and the rock in the central section of the BMT holes and calculated λ (W/m,K) at different times

Time	Hole 1		Hole 2		Hole 3		Hole 4		Hole 5		Hole 6	
	ΔT	λ	ΔT	λ	ΔT	λ	ΔT	λ	ΔT	λ	ΔT	λ
1 week	34	(1.04)	41	0.86	50	0.68	50	0.68	40	0.86	48	0.72
10 weeks	37	0.95	32	1.11	48	0.72	48	0.72	38	0.91	49	0.71
1 year	31	1.14	28	1.27	46	0.75	48	0.72	33	1.04	49	0.71
2.1-3.1 y	26	1.37	24	1.48					29	1.19	46	0.75

The evaluated heat conductivity is shown in Fig. 7-4 for each hole as a function of time from start. There is an obvious difference between the so-called dry and wet holes.

- The heat conductivity of the buffer mass in the dry holes is very low, with a value about 0.7 W/m,K that does not increase with time, which indicates that very little water was taken up.

- The heat conductivity of the wet holes increases with time and ends at values between 1.19 and 1.48 W/m,K showing that water is taken up.

At the excavation of the holes numerous samples were taken and the distribution of the water ratio carefully determined. The average values determined in the central section are for each hole shown in Fig. 7-5 as a function of the distance from the canister surface. The following can be noted from the figure:

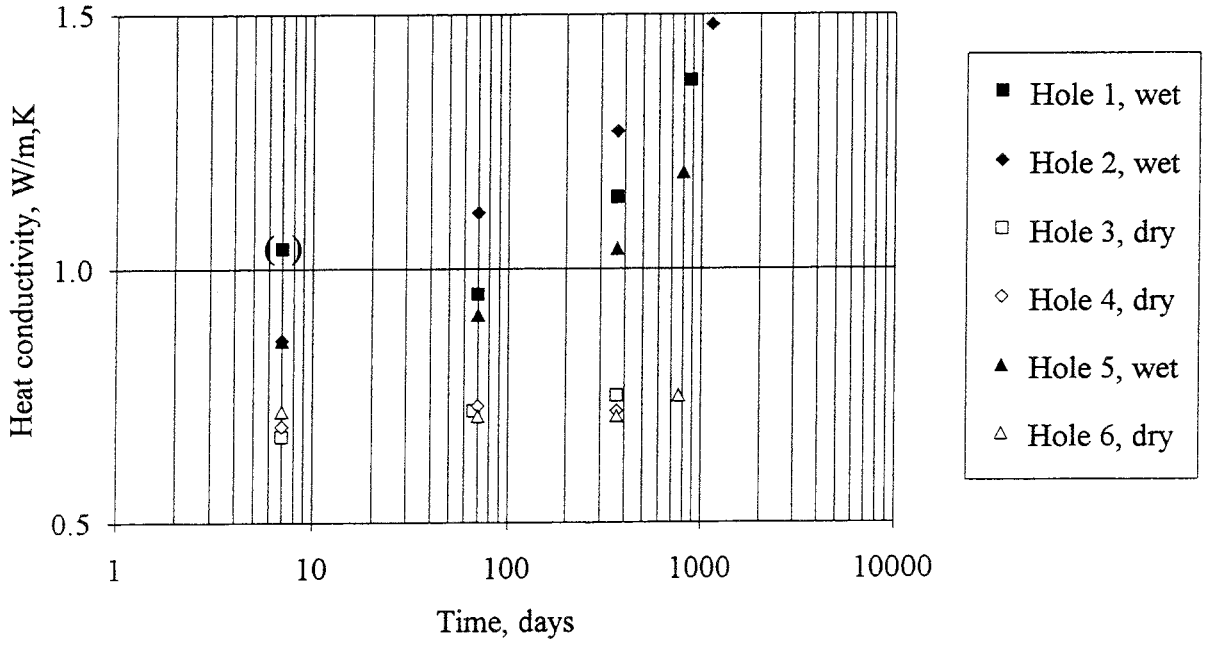

Figure 7-4 Back-calculated average heat conductivity of the buffer material evaluated from BMT as a function of time from emplacement.
Holes 1,2, and 5: Wet holes with 1 cm empty slot at the rock surface.
Holes 3,4, and 6: Dry holes with 3 cm slot filled with uncompacted bentonite at the rock surface

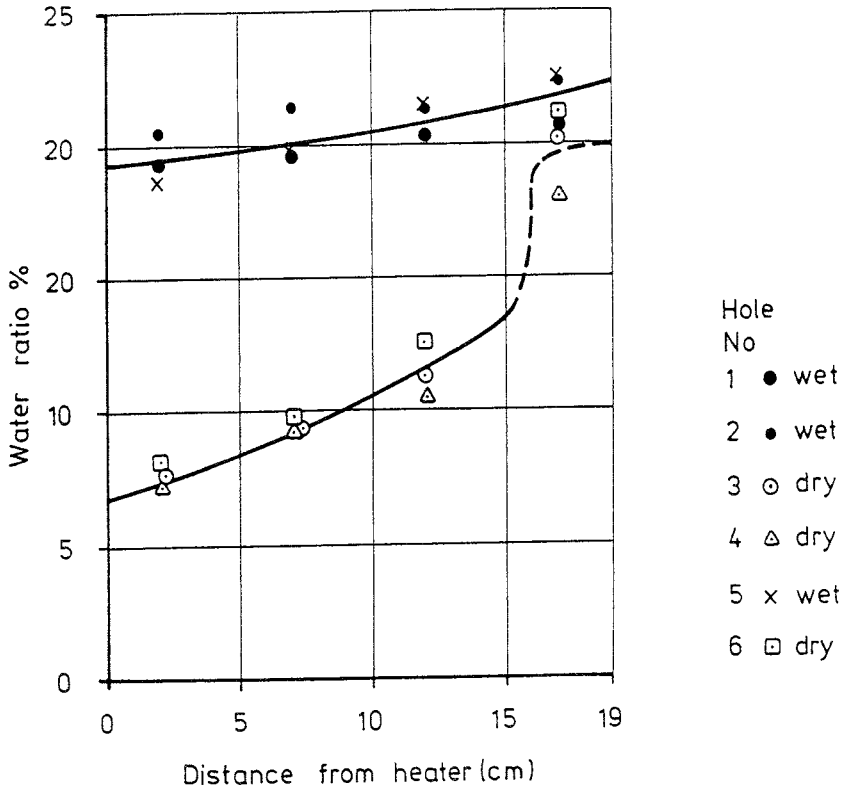

Figure 7-5 Water ratio in the buffer mass at mid height heater as a function of the distance from the heater surface. BMT

- The water ratio gradient in the wet holes was quite small. The water ratio had increased considerably (from 13%) even close to the canister.
- The water ratio gradient in the dry holes was very high and the water ratio had decreased (from 10%) close to the canister.
- The values are remarkably similar for the respective sets of wet and dry holes despite the difference in testing time (0.9 years for hole 4 and 2.1 years for hole 6) and the fact that hole 1 had much higher temperatures before excavation (138°C) due to an increased thermal power to 1400 W during 0.9 years.

The evaluated heat conductivities shown in Fig. 7-4 include the slots at the canisters and at the rock surfaces. An approximate value of the heat conductivity of the blocks can be achieved if the temperature gradient half-way between the rock and the canister is used. Such an evaluation yields λ_c=1.01 W/m,K. The evaluated heat conductivities and the achieved degree of saturation at excavation are shown in Table 7-3.

Table 7-3 Heat conductivity λ of the buffer mass at excavation and the corresponding average degree of saturation S_r and average void ratio e. Index c denotes evaluation of the blocks in the dry holes for the measured temperature gradient half-way between the rock and the canister

Hole No.	λ W/m,K	S_r %	e	λ_c W/m,K	S_{rc} %	e_c
1	1.37	93	0.60			
2	1.48	100	0.60			
3	0.75	56	0.60	1.01	61	0.46
4	0.72	51	0.60	1.01	60	0.46
5	1.19	96	0.60			
6	0.75	60	0.60	1.01	67	0.46

7.4 HEAT CONDUCTIVITY EVALUATED FROM THE SETTLEMENT TEST

The pilot settlement test in Stripa was a 5 year test in a bore hole with 40 cm length and 2.7 m depth, which can also be used for back-calculating the in situ heat conductivity of the buffer material. It was made of highly compacted blocks of Na-bentonite Mx-80. The geometry is shown in Fig. 7-6. The test has been described in detail by Börgesson (1993).

The temperature was measured at the heater surface and close to the rock surface in the central section. Sampling after completed test showed that the buffer material had an average degree of saturation of $S_r = 97\%$, with a somewhat lower value for the the central part. The temperature evolution was calculated applying the heat conductivity $\lambda = 1.4$ W/m,K, but the obtained temperature drop was a little smaller than the measured one and back-calculation resulted in $\lambda = 1.25$ W/m,K. The evaluated data of the buffer mass at the central section were:

$\lambda = 1.24$ W/m,K
$e = 0.88$
$S_r = 95\%$

7.5 HEAT CONDUCTIVITY EVALUATED FROM THE SKB/CEA TEST OF FRENCH CLAY

Two high-temperature tests in drilled holes in Stripa with the French reference clay Fo-Ca can also be used for back-calculating the heat conductivity. The tests, which are described by Pusch et al. (1992), were made in two 2.5 m long bore holes with 0.2 m diameter. The heaters had a length of 1.5 m and were enclosed by steel tubes with a diameter of 51 mm. Since $L/R > 10$, Eqn 7-1 can approximately be used for back-calculating the heat conductivity.

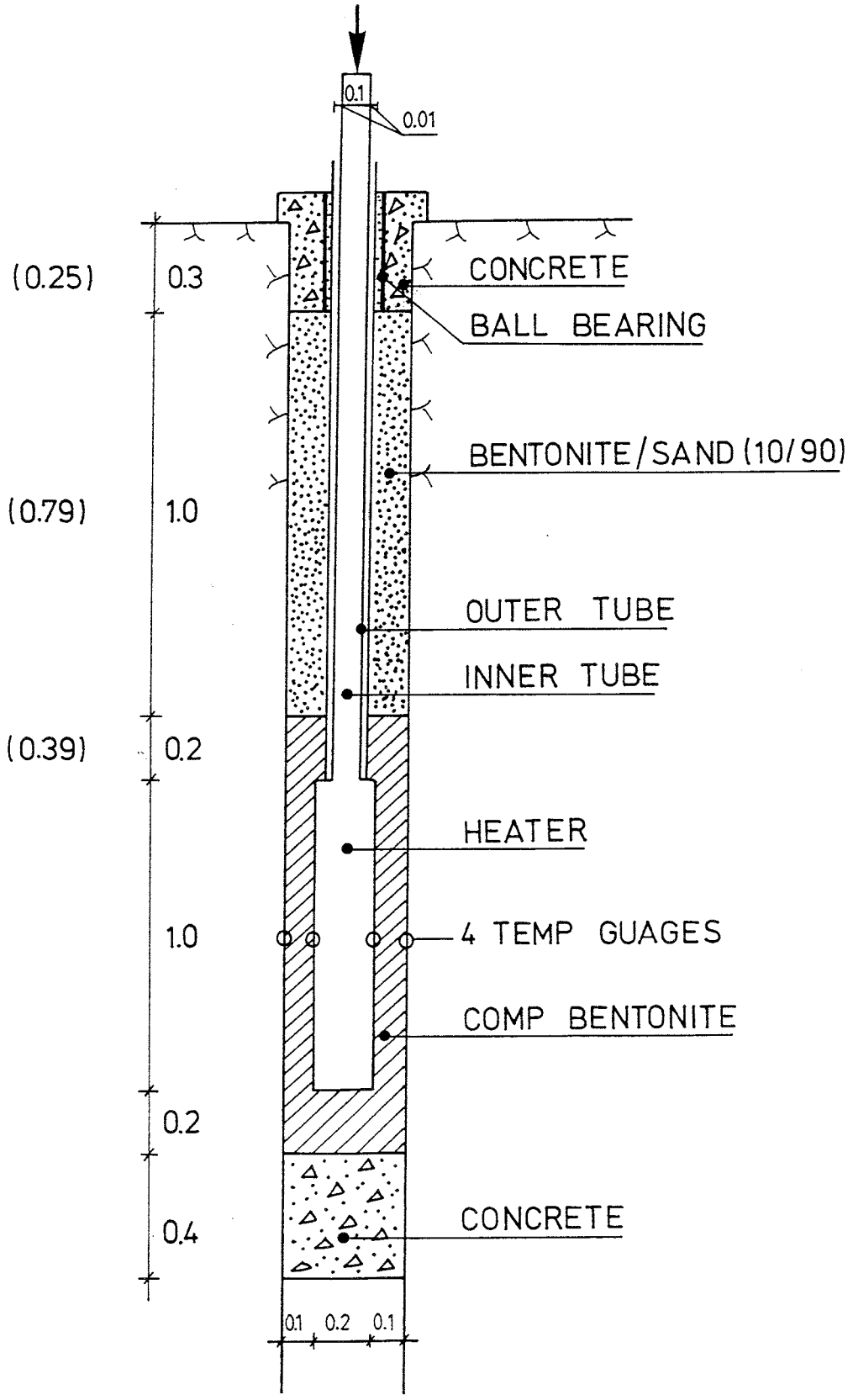

Figure 7-6 Cross section of the deposition hole in the settlement test

The excavation of the clay, which was made after 0.5 and 2 years, respectively, showed that the degree of saturation was $S_r \approx 85\%$ on an average with a dry zone close to the heater (S_r = 50-70%). The temperatures were very high with a maximum value in the buffer of about 170°C.

Hole I could not be evaluated due to uncertainties in the exact location of the thermo-couples. Hole II, which was heated with the power 1 000 W for 2 years, had a temperature drop of 90-95°C between the heater (R_2=0.0255 m) and the outer thermo-couple (R_1 = 0.0935-0.1000 m). The back-calculated conductivity and the measured average data of the buffer at mid height heater are:

$\lambda \approx$ 1.4-1.5 W/m,K
e = 0.82
S_r = 85%

The heat conductivity is probably somewhat overestimated due to the axial conduction of heat in the upper part of the steel tube. The scatter is thus probably:

1.3 W/m,K<λ<1.5 W/m,K.

A more accurate estimation of the heat conductivity requires a detailed calculation.

8 COMPARISONS BETWEEN THE HEAT CONDUCTIVITY EVALUATED FROM THEORETICAL CONSIDERATIONS, LABORATORY MEASUREMENTS, AND BACK-CALCULATIONS

8.1 GENERAL

The heat conductivity of buffer materials has been determined using three different techniques:

- Theoretical derivation according to earlier reports
- Laboratory measurements
- Back calculations from field tests

These results will be compared in this chapter with special respect to the estimated influence of the temperature and pressure.

8.2 COMPARISONS BETWEEN LABORATORY MEASUREMENT AND THEORETICAL EVALUATION OF HEAT CONDUCTIVITY

Influence of degree of saturation

The data in Fig 2-3 obtained by applying the three different methods, and those shown in Fig 6-2 are compared in Fig 8-1. This diagram shows that all the theoretical methods yield values that do not deviate very much from the meaurements. The maximum deviation is about 0.2 W/m,K. However, the diagram also shows that none of the methods seems to reflect the influence of a change in degree of saturation very well. The measured effect of a change in degree of saturation is much larger at $40\%<S_r<60\%$ than at $80\%< S_r<100\%$. Only one of the methods accounts for this effect. It is obvious that none of these methods is sufficiently accurate for predicting the influence of a change in degree of saturation.

Influence of void ratio

Fig 8-2 shows the thermal conductivity evaluated for samples with a degree of saturation of about 50% and close to 100% as a function of the void ratio. The values are plotted together with the theoretical relations according to Fig 2-2. The "saturated samples" had a degree of saturation between 93% and 100 % and the other values, which originally were in the range 40% to 60%, were adjusted to S_r=50% according to the relation in Fig 6-2.

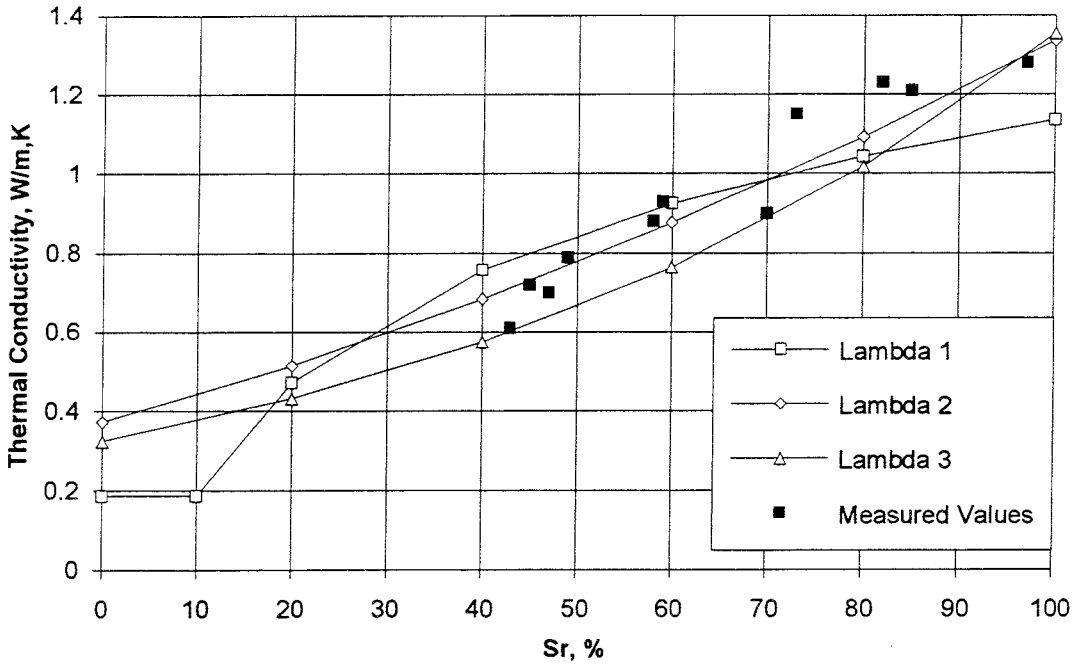

Figure 8-1 Comparison between measured heat conductivity of samples with the void ratio $e \approx 0.8$ and theoretically determined with the three different methods

λ_1 - Knutsson
λ_2 - Kahr et al.
λ_3 - Beziat et al.

The diagram shows that the measured values fall fairly well within the theoretical limits. However, the values measured on samples close to water saturation differ very little in spite of the fairly wide range in void ratio and it is obvious that the number of tests is too small to allow for any definite conclusions concerning the influence of the void ratio on the thermal conductivity.

8.3 COMPARISONS BETWEEN FIELD TESTING AND THEORETICAL EVALUATION OF HEAT CONDUCTIVITY

The heat conductivity evaluated from in-situ tests should be higher than the value obtained from the laboratory tests at room temperature with no confining pressure according to chapter 2. In Table 8-1 the back-calculated heat conductivities from the field tests are "corrected" for the effects of temperature and pressure in order to compare them with the laboratory-derived relations in Fig. 2-2. Correction for temperature is made by taking the average value obtained by applying the two proposed methods and the correction for pressure is made by adding 0.006 W/m,K per MPa pressure according to the results obtained by Knutsson.

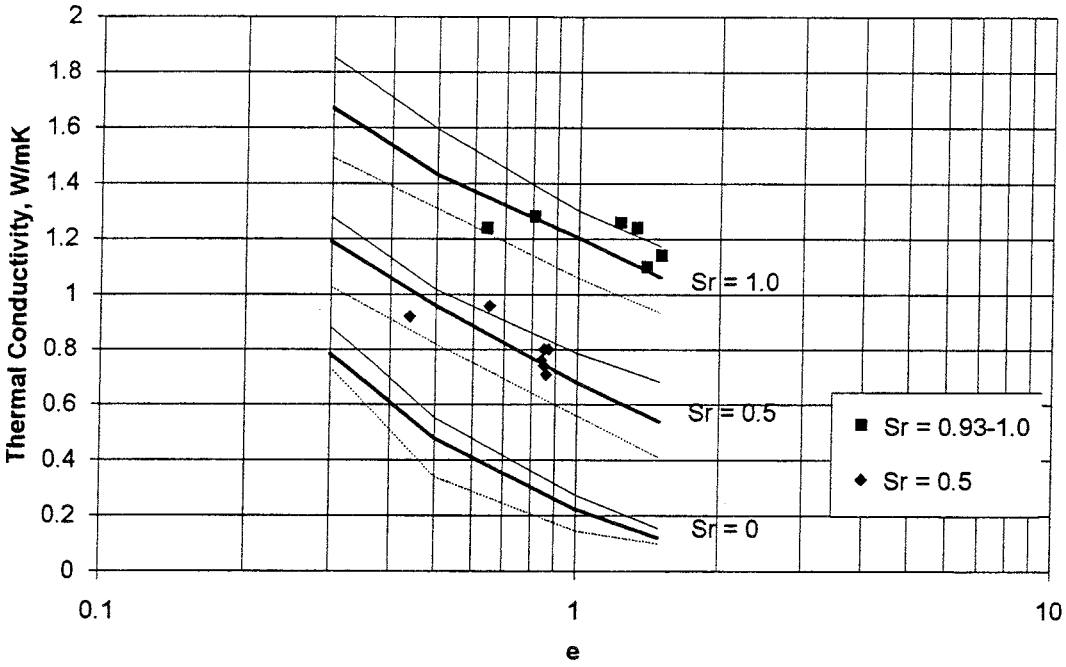

Fig 8-2 Comparison between the measured heat conductivity and the theoretically evaluated (Fig 2-2)

Table 8-1 Heat conductivity back-calculated from the field tests (λ and λ_c) and corrected for temperature and pressure (λ_T).

Test	e	S_r %	λ W/m,K	λ_T W/m,K	Remark
BMT	0.60	96	1.35	1.25	Aver. wet holes
BMT	0.60	56	0.74	0.70	Aver. dry holes
BMT	0.46	63	λ_c=1.01	0.97	Center dry holes
ST	0.88	95	1.25	1.16	
FT	0.82	85	≈1.4	≈1.25	

Fig. 8-3 shows λ and λ_T plotted pair-wise in the same diagram as the theoretically calculated values. The higher values are thus the actual heat conductivities, while the lower values are the corrected ones that would be comparable to the theoretical values if the corrections are valid. The figure shows the following:

- The results from the three wet tests fall fairly well within the expected range although the heat conductivity of the French clay is a little higher and the heat conductivity of Mx-80 at the other two tests a little lower than the respective average theoretical values.

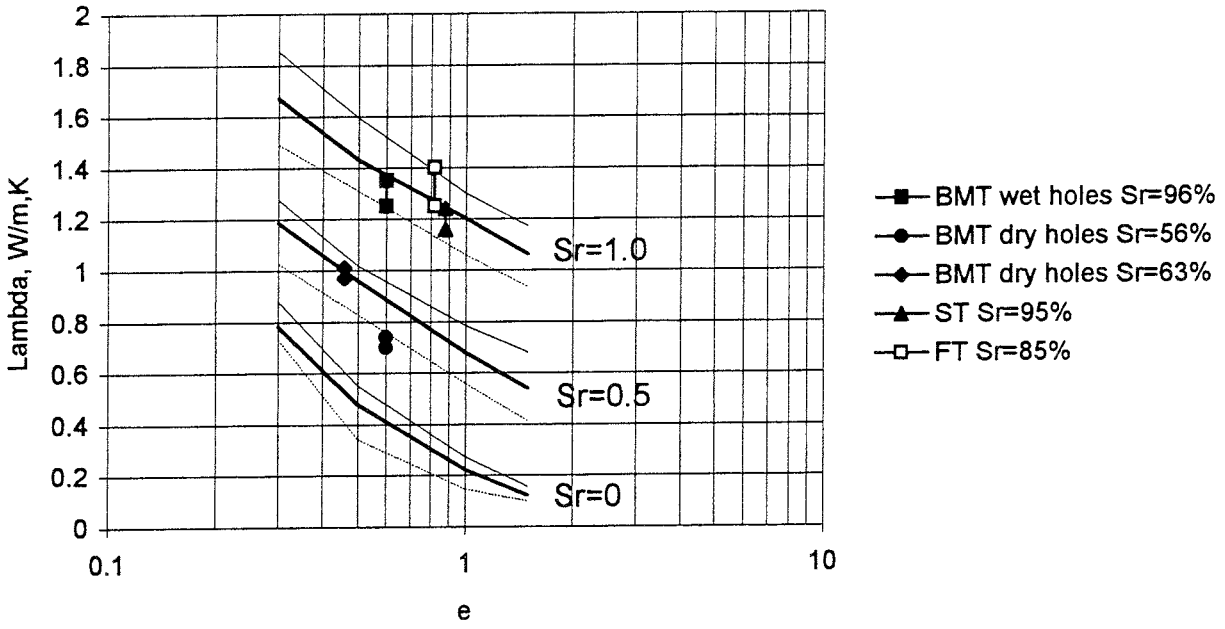

Figure 8-3 Comparison between the heat conductivity evaluated from the three field tests and the expected values. The higher value is the field heat conductivity while the lower value is reduced to correspond to room temperature and no confining pressure

- The heat conductivity of the clay in the centre of the dry holes λ_c is a little lower than expected considering that S_r=64%.
- The average heat conductivity for the dry holes is a little lower than expected.

The values for the dry holes are low in spite of that the condensation-evaporation process has not been taken into account. It can partly be explained in the following way:

- The existence of slots and cracks reduce the heat conductivity.
- The back-calculation is difficult to make since the buffer is rather inhomogeneous both regarding density and degree of saturation.

8.4 INFLUENCE OF THE EVAPORATION-CONDENSATION PROCESS IN A TEMPERATURE GRADIENT

The thermo-hydro-mechanical behaviour of a water-unsaturated clay barriers is very complicated. The temperature gradient in the clay redistributes water from the warmer parts to the colder. The redistribution has the following effects on the thermal conductivity:

- Water vapour is transported along the temperature gradient from the warmer parts to the colder parts. The hot water vapour condenses in the colder part which means that there is also a transportation of heat in the vapour. This effect will thus increase the heat flow and result in an apparent increase in thermal conductivity of the clay.

- The water vapour transport will dry the warmer parts and wet the colder parts. The heat conductivity will thus be lower in the dried parts and higher in the wetted parts.

- The redistribution of water will in some cases cause cracking of the bentonite blocks. This was observed in the dry holes in Stripa. There may thus be a temperature drop across the air-filled cracks and an apparent decrease in thermal conductivity.

The effect of the cracking is very difficult to estimate. The change in thermal conductivity may probably vary from none to 20-30% depending on the direction and width of the cracks.

The effect of the drying and wetting can be estimated if the change in degree of saturation and void ratio is known. According to De Vries (1974) the apparent heat conductivity of pore air increases with temperature due to the evaporation/condensation process. Fig 8-4 shows the change in the apparent heat conductivity of the vapour k_{vs} with temperature. This can be taken into account if the geometric mean model for porous media (Woodside &Messmer, 1961) according to Eqn 8-1 (identical to Eqn 2-3) is applied.

$$\lambda = \lambda_s^{1-n} \cdot \lambda_w^{n \cdot S_r} \cdot \lambda_a^{n \cdot (1-S_r)} \qquad (8\text{-}1)$$

where
λ_s = heat conductivity of solids
λ_w = heat conductivity of water
λ_a = heat conductivity of air
n = porosity (pore volume divided to total volume)
n = $e/(1+e)$
S_r = degree of saturation

Using Eqn 8-1 and the relation between the apparent heat conductivity and the temperature in Fig 8-4 the heat conductivity can be corrected for vapour flow according to Eqns 8-2 and 8-3.

$$\lambda_{cv} = f_{cv} \cdot \lambda \qquad (8\text{-}2)$$

$$f_{cv} = \left(\frac{\lambda_v^T}{\lambda_v^{T_{20}}} \right)^{\frac{e}{1+e}(1-S_r)} \qquad (8\text{-}3)$$

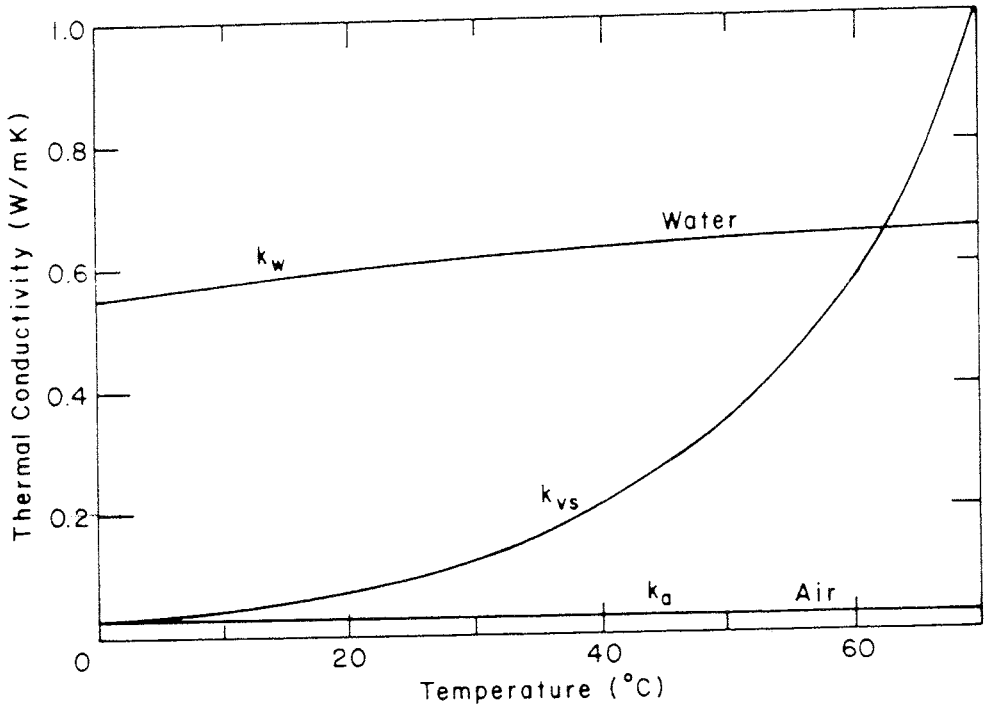

Figure 8-4 Apparent thermal conductivity of pore air k_{vs} due to vapour flow at 1 bar as a function of temperature (De Vries 1974)

where

λ_{cv} = apparent heat conductivity of the buffer material corrected for vapour flow
f_{cv} = correction factor
λ = heat conductivity of the buffer material at T=20°C
$\lambda_v^{T_{20}}$ =heat conductivity of pore air at T=20°C
λ_v^T =apparent heat conductivity of pore air at temperature T

Table 8-2 shows the influence of the vapour flow on the heat conductivities according to Eqns 8-2 and 8-3.

Table 8-2 Heat conductivity λ_r and correction factor f_{cv}.

Test	e	S_r %	λ_r W/m,K	f_{cv}	λ_c/f_{cv}
BMT	0.60	96	1.25	1.02	1.23
BMT	0.60	56	0.70	1.29	0.54
BMT	0.46	63	0.97	1.20	0.80
ST	0.88	95	1.16	1.07	1.08

In order to compare the laboratory data with the field data the heat conductivity must thus be corrected for the pressure and temperature (yields

λ_T according to Table 8-1) as well as the vapour flow by reducing the back-calculated field parameters. By dividing λ_T by f_{cv} the influence of vapour flow is taken into account according to Eqn 8-3. However the heat conductivity of those BMT holes that had a buffer with low degree of saturation will be very low and differ substantially from the theoretical values. The reason for the disagreement is probably either that the correction according to Eqn 8-3 is wrong or that air filled slots and cracks in the buffer have a very large influence on the heat transport.

The processes of heat and moisture flow in unsaturated buffer materials are thus very complicated and not enough well known. The simple correction of the average heat conductivity for moisture flow according to Eqn 8-3 cannot be made if the buffer contains slots or cracks.

9 CONCLUSIONS

In this study a technique for standard testing has been investigated and further developed, and theoretical as well as laboratory-measured values have been compared with values back-calculated from field tests. The following main conclusions can be drawn:

- All laboratory measurements and back-calculations of data from field tests on buffer materials suitable for the KBS3 repository and with void ratios in the range $0.6<e<0.9$ (corresponding to the density at saturation $1.9\ t/m^3<\rho<2.1\ t/m^3$), and a degree of saturation higher than 90%, have yielded a heat conductivity between 1.25 W/m,K and 1.35 W/m,K.

- The three theoretically derived expressions for evaluating the heat conductivity have - for the same range in void ratio - resulted in values between 1.1 W/m,K and 1.5 W/m,K.

- The probe technique for laboratory measurement of the heat conductivity seems to yield results with an accuracy of about ±10% if the proposed techniques for measuring and evaluation are applied.

- The influence of void ratio on the heat conductivity can be fairly well predictable by using the theoretical relations shown in Fig 2-2, but additional measurements are required for safe prediction. The influence of the degree of saturation was not very well predicted using theoretical expressions. It is preferably estimated by the measured relation shown in Fig 6-2.

- The evaluation of the heat conductivity from the field tests showed that the agreement between the laboratory-measured and theoretical values was fairly good when the buffer material was nearly saturated, while the agreement was less good for low degrees of water saturation.

- The investigation gave no evidence that the heat conductivity increases with increasing temperature and pressure as suggested by Knutsson (1983) and Kahr et al. (1982). Further investigations are required before it can be decided if these effects should and can be included in heat calculations.

- For buffer with a low average degree of saturation it was not possible to take into account either the influence of slots, cracks or moisture flow. These effects seem to balance each other to some extent but more investigations would be required in order to understand the processes.

REFERENCES

Beziat A., Dardaine M. and Gabis V., 1988. Effect of compaction pressure and water content on the thermal conductivity of some natural clays. Clays & Clay Minerals 36 (5).

Börgesson L., 1982. BUFFER MASS TEST - Predictions of the behavior of the bentonite-based buffer materials. Stripa Project Internal Report 82-08.

Börgesson L., 1993. Interim report on the pilot settlement test in Stripa. SKB Arbetsrapport (in print)

Farouki O.T., 1986. Thermal Properties of Soils. Trans Tech Publications.

Kahr G. and Müller-von Moos M., 1982. Wärmeleitfähigkeit von Bentonit MX80 und von Montigel nach der Heizdrahtmethode. NAGRA Technischer Bericht 82-06

Karnland O., Sandén T. and Pusch R., 1992. Karakterisering av buffertmaterial. SKB arbetsrapport (in print)

Knutsson S., 1983. On the thermal conductivity and thermal diffusivity of highly compacted bentonite. SKB Technical Report 83-72

Pusch R., Nilsson J. and Ramqvist G., 1985. Final Report of the Buffer Mass Test - Volume I: scope, preparative field work, and test arrangement. Stripa Project Technical Report 85-11

Pusch R., Börgesson L. and Ramqvist G., 1985. Final Report of the Buffer Mass Test - Volume II: test results. Stripa Project Technical Report 85-12.

Pusch R., Karnland O., Lajudie A., Lechelle J. and Bouchet A., 1993. Hydrothermal field test with French candidate clay embedding steel heater in the Stripa mine. SKB Technical Report. 93-02.

Svemar C., and Börgesson L., 1993. Impact of buffer mass thermal properties on repository design - KBS-3 case. International workshop on thermo-mechanics of clays and clay barriers. Bergamo.

Woodside W. and Messmer J.M., 1961. Thermal conductivity of porous media. Journal of Applied Physics, vol. 32, No. 9.

List of SKB reports

Annual Reports

1977-78
TR 121
KBS Technical Reports 1 – 120
Summaries
Stockholm, May 1979

1979
TR 79-28
The KBS Annual Report 1979
KBS Technical Reports 79-01 – 79-27
Summaries
Stockholm, March 1980

1980
TR 80-26
The KBS Annual Report 1980
KBS Technical Reports 80-01 – 80-25
Summaries
Stockholm, March 1981

1981
TR 81-17
The KBS Annual Report 1981
KBS Technical Reports 81-01 – 81-16
Summaries
Stockholm, April 1982

1982
TR 82-28
The KBS Annual Report 1982
KBS Technical Reports 82-01 – 82-27
Summaries
Stockholm, July 1983

1983
TR 83-77
The KBS Annual Report 1983
KBS Technical Reports 83-01 – 83-76
Summaries
Stockholm, June 1984

1984
TR 85-01
Annual Research and Development Report 1984
Including Summaries of Technical Reports Issued during 1984. (Technical Reports 84-01 – 84-19)
Stockholm, June 1985

1985
TR 85-20
Annual Research and Development Report 1985
Including Summaries of Technical Reports Issued during 1985. (Technical Reports 85-01 – 85-19)
Stockholm, May 1986

1986
TR 86-31
SKB Annual Report 1986
Including Summaries of Technical Reports Issued during 1986
Stockholm, May 1987

1987
TR 87-33
SKB Annual Report 1987
Including Summaries of Technical Reports Issued during 1987
Stockholm, May 1988

1988
TR 88-32
SKB Annual Report 1988
Including Summaries of Technical Reports Issued during 1988
Stockholm, May 1989

1989
TR 89-40
SKB Annual Report 1989
Including Summaries of Technical Reports Issued during 1989
Stockholm, May 1990

1990
TR 90-46
SKB Annual Report 1990
Including Summaries of Technical Reports Issued during 1990
Stockholm, May 1991

1991
TR 91-64
SKB Annual Report 1991
Including Summaries of Technical Reports Issued during 1991
Stockholm, April 1992

1992
TR 92-46
SKB Annual Report 1992
Including Summaries of Technical Reports Issued during 1992
Stockholm, May 1993

1993
TR 93-34
SKB Annual Report 1993
Including Summaries of Technical Reports Issued during 1993
Stockholm, May 1994

Technical Reports
List of SKB Technical Reports 1994

TR 94-01
Anaerobic oxidation of carbon steel in granitic groundwaters: A review of the relevant literature
N Platts, D J Blackwood, C C Naish
AEA Technology, UK
February 1994

TR 94-02
Time evolution of dissolved oxygen and redox conditions in a HLW repository
Paul Wersin, Kastriot Spahiu, Jordi Bruno
MBT Technología Ambiental, Cerdanyola, Spain
February 1994

TR 94-03
Reassessment of seismic reflection data from the Finnsjön study site and prospectives for future surveys
Calin Cosma[1], Christopher Juhlin[2], Olle Olsson[3]
[1] Vibrometric Oy, Helsinki, Finland
[2] Section for Solid Earth Physics, Department of Geophysics, Uppsala University, Sweden
[3] Conterra AB, Uppsala, Sweden
February 1994

TR 94-04
Final report of the AECL/SKB Cigar Lake Analog Study
Jan Cramer (ed.)[1], John Smellie (ed.)[2]
[1] AECL, Canada
[2] Conterra AB, Uppsala, Sweden
May 1994

TR 94-05
Tectonic regimes in the Baltic Shield during the last 1200 Ma - A review
Sven Åke Larsson[1,2], Eva-Lena Tullborg[2]
[1] Department of Geology, Chalmers University of Technology/Göteborg University
[2] Terralogica AB
November 1993

TR 94-06
First workshop on design and construction of deep repositories - Theme: Excavation through water-conducting major fracture zones Såstaholm Sweden, March 30-31 1993
Göran Bäckblom (ed.), Christer Svemar (ed.)
Swedish Nuclear Fuel & Waste Management Co, SKB
January 1994

TR 94-07
INTRAVAL Working Group 2 summary report on Phase 2 analysis of the Finnsjön test case
Peter Andersson (ed.)[1], Anders Winberg (ed.)[2]
[1] GEOSIGMA, Uppsala, Sweden
[2] Conterra, Göteborg, Sweden
January 1994

TR 94-08
The structure of conceptual models with application to the Äspö HRL Project
Olle Olsson[1], Göran Bäckblom[2], Gunnar Gustafson[3], Ingvar Rhén[4], Roy Stanfors[5], Peter Wikberg[2]
1 Conterra AB
2 SKB
3 CTH
4 VBB/VIAK
5 RS Consulting
May 1994

TR 94-09
Tectonic framework of the Hanö Bay area, southern Baltic Sea
Kjell O Wannäs, Tom Flodén
Institutionen för geologi och geokemi, Stockholms universitet
June 1994

TR 94-10
Project Caesium–An ion exchange model for the prediction of distribution coefficients of caesium in bentonite
Hans Wanner[1], Yngve Albinsson[2], Erich Wieland[1]
[1] MBT Umwelttechnik AG, Zürich, Switzerland
[2] Chalmers University of Technology, Gothenburg, Sweden
June 1994

TR 94-11
Äspö Hard Rock Laboratory Annual Report 1993
SKB
June 1994

TR 94-12
Research on corrosion aspects of the Advanced Cold Process Canister
D J Blackwood, A R Hoch, C C Naish, A Rance, S M Sharland
AEA Technology, Harwell Laboratory, UK
January 1994

TR 94-13
Assessment study of the stresses induced by corrosion in the Advanced Cold Process Canister
A R Hoch, S M Sharland
Chemical Studies Department, Radwaste Disposal Division, AEA Decommissioning and Radwaste, Harwell Laboratory, UK
October 1993

TR 94-14
Performance of the SKB Copper/Steel Canister
Hans Widén[1], Patrik Sellin[2]
[1] Kemakta Konsult AB, Stockholm, Sweden
[2] Svensk Kärnbränslehantering AB, Stockholm, Sweden
September 1994

TR 94-15
Modelling of nitric acid production in the Advanced Cold Process Canister due to irradiation of moist air
J Henshaw
AEA Technology, Decommissioning & Waste Management/Reactor Services, Harwell, UK
January 1994

TR 94-16
Kinetic and thermodynamic studies of uranium minerals. Assessment of the long-term evolution of spent nuclear fuel
Ignasi Casas[1], Jordi Bruno[1], Esther Cera[1], Robert J Finch[2], Rodney C Ewing[2]
[1] MBT Tecnología Ambiental, Cerdanyola, Spain
[2] Department of Earth and Planetary Sciences, University of New Mexico, Albuquerque, NM, USA
October 1994

TR 94-17
Summary report of the experiences from TVO's site investigations
Antti Öhberg[1], Pauli Saksa[2], Henry Ahokas[2], Paula Ruotsalainen[2], Margit Snellman[3]
[1] Saanio & Riekkola Consulting Engineers, Helsinki, Finland
[2] Fintact Ky, Helsinki, Finland
[3] Imatran Voima Oy, Helsinki, Finland
May 1994

TR 94-18
AECL strategy for surface-based investigations of potential disposal sites and the development of a geosphere model for a site
S H Whitaker, A Brown, C C Davison, M Gascoyne, G S Lodha, D R Stevenson, G A Thorne, D Tomsons
AECL Research, Whiteshell Laboratories, Pinawa, Manitoba, Canada
May 1994

TR 94-19
Deep drilling KLX 02. Drilling and documentation of a 1700 m deep borehole at Laxemar, Sweden
O Andersson
VBB VIAK AB, Malmö
August 1994

TR 94-20
Technology and costs for decommissioning the Swedish nuclear power plants
Swedish Nuclear Fuel and Waste Management Co, Stockholm, Sweden
June 1994

TR 94-21
Verification of HYDRASTAR: Analysis of hydraulic conductivity fields and dispersion
S T Morris, K A Cliffe
AEA Technology, Harwell, UK
October 1994

TR 94-22
Evaluation of stationary and non-stationary geostatistical models for inferring hydraulic conductivity values at Äspö
Paul R La Pointe
Golder Associates Inc., Seattle, WA, USA
November 1994

TR 94-23
PLAN 94
Costs for management of the radioactive waste from nuclear power production
Swedish Nuclear Fuel and Waste Management Co
June 1994

TR 94-24
Äspö Hard Rock Laboratory Feasibility and usefulness of site investigation methods. Experiences from the pre-investigation phase
Karl-Erik Almén (ed.)[1], Pär Olsson[2], Ingvar Rhén[3], Roy Stanfors[4], Peter Wikberg[5]
[1] KEA GEO-Konsult
[2] SKANSKA
[3] VBB/VIAK
[4] RS Consulting
[5] SKB
August 1994

TR 94-25

Kinetic modelling of bentonite-canister interaction. Long-term predictions of copper canister corrosion under oxic and anoxic conditions

Paul Wersin, Kastriot Spahiu, Jordi Bruno
MBT Tecnología Ambiental, Cerdanyola, Spain
September 1994

TR 94-26

A surface chemical model of the bentonite-water interface and its implications for modelling the near field chemistry in a repository for spent fuel

Erich Wieland[1], Hans Wanner[1], Yngve Albinsson[2], Paul Wersin[3], Ola Karnland[4]
[1] MBT Umwelttechnik AG, Zürich, Switzerland
[2] Chalmers University of Technology, Gothenburg, Sweden
[3] MBT Tecnología Ambiental, Cerdanyola, Spain
[4] Clay Technology AB, Lund, Sweden
July 1994

TR 94-27

Experimental study of strontium sorption on fissure filling material

Trygve E Eriksen, Daqing Cui
Department of Chemistry, Nuclear Chemistry, Royal Institute of Technology, Stockholm, Sweden
December 1994

TR 94-28

Scenario development methodologies

Torsten Eng[1], John Hudson[2], Ove Stephansson[3], Kristina Skagius[4], Marie Winborgh[4]
[1] Swedish Nuclear Fuel & Waste Management Co, Stockholm, Sweden
[2] Rock Engineering Consultants, Welwyn Garden City, Herts, UK
[3] Div. of Engineering Geology, Royal Institute of Technology, Stockholm, Sweden
[4] Kemakta, Stockholm, Sweden
November 1994